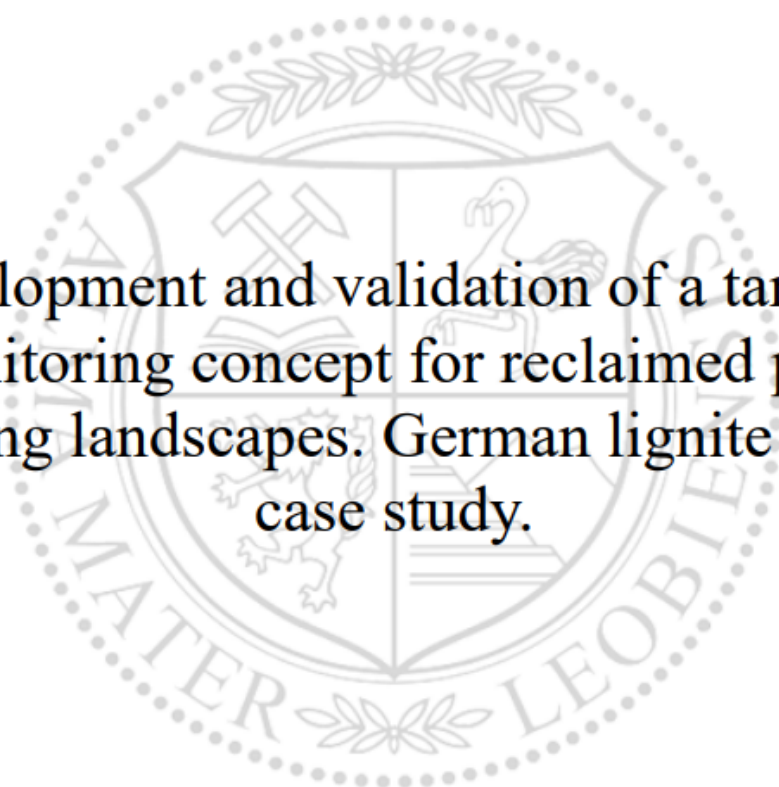




Chair of Mining Engineering and Mineral Economics

Master's Thesis



Development and validation of a targeted monitoring concept for reclaimed post-mining landscapes. German lignite mine case study.

Paulina Loskot

April 2023



AFFIDAVIT

I declare on oath that I wrote this thesis independently, did not use other than the specified sources and aids, and did not otherwise use any unauthorized aids.

I declare that I have read, understood, and complied with the guidelines of the senate of the Montanuniversität Leoben for "Good Scientific Practice".

Furthermore, I declare that the electronic and printed version of the submitted thesis are identical, both, formally and with regard to content.

Date 27.03.2023

A handwritten signature in cursive script, appearing to read 'Paulina Loskot', written over a horizontal line.

Signature Author
Paulina Loskot

Table of Contents

List of abbreviations:.....	5
1. Introduction.....	6
1.1. Background and motivation.....	6
1.2. Objective.....	6
1.3. Scope of the study.....	6
2. State-of-the-art	7
2.1. Mining and Post-mining Landscapes	7
2.1.1. Impact of mining	7
2.1.2. Post-mining landscape.....	8
2.2. Reclamation.....	8
2.2.1. Stages of reclamation	8
2.2.2. Types of reclamation.....	9
2.3. Mining Law and Federal Nature Conservation Law	9
2.4. Sustainable development (in mining).....	10
2.5. European directives	11
2.6. Monitoring.....	11
2.6.1. Remote Sensing.....	12
2.6.2. Satellite missions.....	12
2.6.3. Future satellite missions	18
2.7. Environmental monitoring.....	19
2.7.1. Environmental indices.....	19
2.7.2. Monitoring of surface mining	19
2.7.3. Spectral indexes.....	19
2.7.4. Recent publications on spectral indexes application.....	21
2.8. Reclamation monitoring methods in recent publications	27
2.9. Summary.....	29
3. Data requirement and methodology	29
3.1. Data acquisition	29
3.2. Processing.....	29
3.3. Indexes.....	30
4. Input data.....	32
4.1. Satellite data	32
4.1. Study area	33
4.2. Droughts in Germany	36

5. Result analyses.....	37
5.1. Indices statistics	37
5.1.1. Monthly statistics.....	41
5.1.2. Monthly statistics for single zone points	45
5.1.3. Differential rasters	47
5.1.4. Discussion.....	49
6. Conclusions.....	49
7. Future recommendations.....	51
8. Bibliography	51
List of Figures.....	58
List of Tables	59
List of Appendices	59

List of abbreviations:

ASTER – Advanced Spaceborne Thermal Emission and Reflection

CAVIS – Clouds, Aerosols, Vapours, Ice and Snow

CSRD – Corporate Sustainability Reporting Directive

ESG – Environment, Social and Governance

ESRS – European Sustainability Reporting Standards

ETM+ – Enhanced Thematic Mapper

FSDU – Forest spatial division units

GIS – Geographic information system

GPS – Global Positioning System

GRI – Global Reporting Initiative

MS – multispectral

MSS – Multi-Spectral Scanner

NFRD – Non-financial Reporting Directive

NIR – near infrared

OLI – Operational Land Imager

PAN – panchromatic

PCA – Principle Component Analysis

RS – remote sensing

SD – Sustainable Development

SDG – Sustainable Development Goals

SFDR – Sustainable Finance Disclosure Regulation

SWIR – shortwave infrared

TCFD – Task Force on Climate-Related Financial Disclosures

TIRS – Thermal Infrared Sensor

TM – Thematic Mapper

VNIR – visible near-infrared

VRE – Vegetation red edge

1. Introduction

1.1. Background and motivation

Mining activities negatively affect the environment, requiring monitoring both during and after mining. The nature of these effects varies substantially depending on the mining methods used. For opencast mining, such as lignite mining, the main problem is land occupation, particularly agricultural and forest land. Another issue that needs to be addressed is mining drainage, resulting in environmental degradation and large-scale changes in land use. After closing such mines there is always post-mining land that has to be taken care of.

European Union laws require large companies to disclose information on the way they operate and manage social and environmental challenges. One of the company's requirements is to provide detailed reports on the environmental impacts, which might be production of carbon dioxide, water contamination or land degradation. Improving monitoring of rehabilitated landscapes, that were once mining areas, would help meet European standards.

It's important to constantly monitor the condition of a given area, and right now it is starting to get easier with the help of remote sensing. These past two decades, there was a significant increase in the technical level of remote sensing methods and computational techniques, which dramatically expanded the possibilities of remote study of phenomena occurring in the environment, both natural and anthropogenic. Remote sensing data is now widely available. With the help of observation programme such as Copernicus Land Monitoring Service all information is free and openly accessible to all users, as it provides geographical information on land cover, land use, land cover-use changes over the years, vegetation state or water cycle.

1.2. Objective

The purpose of this study is to research suitable satellite based spectral indexes with the intention to use them for designing a project workflow that would be useful for monitoring the health and condition of (reclaimed) post-mining landscapes. The study will be carried out on a chosen opencast mine located in Profen, Germany. The research will focus on Landsat satellite data and multispectral imagery. The condition of the post-mining landscape will be determined by an analysis of vegetation indexes in time for selected post-mining test zones.

1.3. Scope of the study

The whole study is divided into two parts. The first, theoretical part consists of a literature study associated with sustainable development, mining and reclamation. In addition, a large section of the theoretical part is devoted to a comprehensive review of satellite missions and multispectral bands registered by their sensors, but also on spectral indexes that can be helpful with establishing the condition of the land. The second part introduces a case study in Profen, Germany. The knowledge acquired in the theoretical part will be used to develop and test a methodological workflow for monitoring postmining landscape health. The condition of the post-mining landscape would be assessed by time series analysis. Monitoring would be conducted in QGIS, which is free and open-source software.

2. State-of-the-art

2.1. Mining and Post-mining Landscapes

The mining industry is considered to have one of the most detrimental impacts on the environment. Extraction of minerals often results in irreversible changes. This chapter discusses the impact of mining on the environment and describes post-mining areas.

2.1.1. Impact of mining

Mineral extraction is influencing the environment in various ways. The noticeable negative effects are bad air quality, water and soil contamination, disturbance of the groundwater table level and negative impact on people's health. In addition, it has negative impact on the development of agriculture, deterioration of the landscape and loss of forest and biodiversity. To understand how and why mining affects the environment so much, it is important to understand the basic processes involved in the extraction and processing of minerals and at what stages environmental impacts can occur (Jain et al., 2016). Figure 1 presents a chart with simplified mining operations.



Figure 1. Simplified flow chart of a surface mining operations

In the exploration phase information about the location and value of the mineral ore deposit is obtained, by performing surveys, field studies and drilling boreholes. In this case, clearing the vegetation is an indispensable process.

The development of the mine may consist of the construction of access roads and mining facilities, for that there has to be carried out site preparation and land clearing. It brings stress to ecologically sensitive areas, increased traffic volumes and general stress related to development activities.

Where the ore deposit extends from the surface deep into the ground, removal of the overburden has to be performed, as well as drilling and blasting to initiate open pit mining. Getting rid of the overburden is destroying natively vegetated areas. Due to this, surface mining is the most environmentally-destructive type of mining, especially within tropical rainforests, it has a huge impact on wildlife habitats.

In some cases, when the open pit mine extends below the groundwater table, the groundwater must be pumped permanently out of the pit to allow mining activities. As a result, a pit lake will form after the mine is closed.

As stated, before overburden must be excavated to allow access to the orebody, consequently waste rocks are being dumped on the mining site, creating piles on the surface, at times containing significant levels of toxic substances.

Extraction of the orebody with specialized equipment by drilling and blasting, followed by transport of material to processing facilities with e.g., loaders, creates a unique set of environmental impacts depending on the ore type, mine type and mining method. These impacts can be air (particle) pollution, excessive noise, vibrations and shock waves.

Activities such as crushing, separation or flotation, that make up the enrichment, contribute to air pollution, creation of tailings or dump leach residuals. The beneficiation processes generate high-volume waste, that usually contain toxic metals (Pb, As, Cd). A mining project which involves the extraction of some hundred million tons of ore minerals, involves also the generation of a similar quantity of tailings. Mine tailings also pose a risk of acid mine drainage and subsequent water contamination (ELAW - Environmental Law Alliance Worldwide, 2010).

2.1.2. Post-mining landscape

The term post-mining landscape generally refers to the cultural landscape that is created or developed in large-scale areas of mining during mining or after its end, during reclamation processes. A distinction must be made between the mining landscape and the post-mining landscape. According to the technical definition, the post-mining landscape is a mining landscape that has been released from mining control, regardless of whether and how many technical measures have taken place to restore near-natural habitats. The post-mining landscape has to be transferred to a reusable state.

2.2. Reclamation

Every mining company will sooner or later have to end its mining activity. The process of renewal of such areas by natural reclamation could take a very long time, therefore reclamation is an element of spatial management, which results in restoring the values and most often assigning a new purpose to the areas transformed by mining.

For all mines, land reclamation should be carried out as the land becomes redundant for mining operations. Therefore, there is no need to wait for the end of mining, but it is even necessary to recultivate areas where mining activity has been completed at the stage of exploitation. All activities should be specified at the beginning stage of a mine. In Poland it is specified as a reclamation project, which is a technical document that assumes the performance of specific works aimed at restoring utility or natural values to land that has been degraded or devastated (Krzemiński, 2021).

Not only areas where the extraction took place are subject to reclamation - these are also soils or water reservoirs, which are often contaminated as a result of industrial activity, e.g., with heavy metals.

2.2.1. Stages of reclamation

From ecological perspective reclamation is the process of construction of topographic, soil and plant conditions that are not identical but permits the degraded landmass to function adequately in the ecosystem of which it was and is part.

Recultivation refers to technically and materially complex measures to restore or return a landscape to a usable state, which has been impaired or destroyed by massive interventions as a result of human economic activities.

Land recultivation is carried out in two stages:

1. Technical recultivation consists of levelling the surface, ground re-contouring, removing or neutralizing toxic substances for plants, constructing reclamation and other structures, including drainage systems.

2. Biological reclamation consists of measures aimed at restoration of soil fertility on technically prepared areas, including agrotechnical and phytomeliorative methods aimed at restoration of flora and fauna (revegetation and seeding), but also initial planting.

Simultaneously with the changes caused by reclamation, there has to be constant monitoring of the soil and water quality and vegetation establishment (*Land Reclamation in Canada | Land Reclamation Projects & Action | CAPP*, n.d.)(*Land Recultivation * Arable Farming*, n.d.).

2.2.2. Types of reclamation

The newly created or restored cultural landscapes are planned and mostly serve subsequent uses. There are different ways of reclamation that can be applied to various circumstances, for example:

- agriculture for cropping and breeding animals,
- forestry to help increase forest resources and plantation, protect endangered species,
- aquatic, increasing water areas, water retention and regulation, recreation,
- natural for preserving, proper use and recreating natural resources, especially wildlife vegetation and animals, ecosystems,
- economic for expanding industrial, communal and service as well as recreational and sports areas,
- cultural to preserve and promote artistic objects (Kasprzyk, 2009).

The selection of the way for reclamation-specific areas is guided by the opinion of the public, investors and officials. It is also conditioned by environmental factors.

2.3. Mining Law and Federal Nature Conservation Law

Reclamation of lignite mines and dumps in Germany began in the early twentieth century, but the progress of these activities was very slow compared with the creation of newly disturbed areas at an ever-increasing rate. This is why the Federal Mining Law (Bundesberggesetz, BBergG) was adopted in 1980, which began regulating all aspects of mining, from extraction to closure and reclamation of mines. This law was also integrated and applied in the new “east” federal states after the reunification of Germany in 1989 (Tymchuk et al., 2021). The BBergG requires mine operators to submit reclamation plans and to carry out reclamation measures on time. These measures may include soil stabilization, vegetation restoration, and water management.

Companies linked to mining (coking plants, chemical plants etc.) are also regulated by several environmental and area planning laws. The most significant of them is the Federal Soil Protection Act (Bundesbodenschutzgesetz). It obliges the originator to clean up contaminated sites. If remedial measures are necessary, the polluter is responsible for preparing the reclamation analysis and the reclamation plan (Wirth & Lintz, 2006).

Another important aspect of mining and environmental law in Germany is monitoring. The BImSchG (Bundes-Immissionsschutzgesetz) requires mine operators to conduct regular monitoring of the environmental impacts of their operations, such as air and water quality, noise levels, and land use changes. This monitoring is used to ensure that mining operations are not causing significant harm to the environment and to identify any issues that may need to be addressed. According to § 15 Abs. 4 BNatSchG (Bundesnaturschutzgesetz), compensatory and replacement measures must be secured and, if necessary, maintained by the polluter or his legal successor for the period required in each case. In addition, the effectiveness of the measures must be verified by monitoring (Knipfer & Schierack, 2018).

Overall, mining and environmental law in Germany is designed to balance the economic benefits of mining with the protection of the environment and the health and well-being of local communities. The laws place strict requirements on mine operators to ensure that mining activities are conducted in an environmentally responsible manner and that the land is properly reclaimed after mining is completed.

2.4. Sustainable development (in mining)

The concept of sustainable development was introduced in 1980, by the ‘International Union for Conservation of Nature and Natural Resources’ (IUCN). In the report “strategies to preserve natural resources”, they used the term SD to define the situation that isn’t damaging for nature, on the contrary, supports it. In addition, this concept was introduced with the approach of the World Commission on Environment and Development (WCED) in 1987. It was only in the 1990s that social and economic aspects were added to the SD principle (Asr et al., 2019). Perhaps the best expression for SD is the definition proposed by the Brundtland Commission: “Sustainable development is development that meets the needs of the present without compromising the ability of future generations to meet their own needs.” Therefore, SD is a development plan that not only considers improving the life of the present generation but also future generations (Cerin, 2006), (Dernbach, 2003), (Dernbach, 1998), (Asr et al., 2019).

Each year, there is an increasing amount of discussion about sustainable development in mining. An ideal goal of sustainable development of mineral resources is to maintain a balance between the development of the economy, the protection of the environment, the benefits to the local community, and the responsibilities of the government as a whole. The extraction of minerals from the earth presents opportunities, challenges and risks to sustainable development. The Agenda 2030 for Sustainable Development of the United Nations concerns, among other things, the minimization of negative mining impacts (*Transforming Our World: The 2030 Agenda for Sustainable Development* | Department of Economic and Social Affairs, n.d.). Reclamation, responsible for reviving damaged and contaminated post-mining areas should be seen as a process that contributes to the achievement of the Sustainable Development Goals (Kretschmann, 2020).

‘Sustainability Schemes for Mineral Resources: A Comparative Overview’ made several recommendations related to the development of standards on sustainability issues for which guidance is still lacking. For instance, sustainability in mining is more often

included in programs and references are used for legitimation, when international guidance documents and norms are available, such as the International Labour Organization (ILO) Conventions and Recommendations. Still, some sub-issues in the areas of environment, social welfare and company governance are not addressed and are less frequently included in the systems. There is a need to analyze in which areas international guidance documents are missing and could contribute to the development of standards and schemes. In addition, mining-specific issues such as site closures and reclamation may require mining guidelines, which are already provided by some mining associations. Moreover, mining standards on specific sub-issues such as sustainability reporting (Global Reporting Initiative – GRI) and safe handling of cyanide (cyanide code) are referenced by several programs, indicating that they help standardize systems issues (Kickler & Franken, 2017).

According to (*OCP Group - Sustainability Integrated Report, 2021*) some of the sustainable goals connected with reclamation might be the ambition to accelerate the rate of rehabilitation in the coming years to cover most of the land exploited in the past, choosing the most suitable crops for the disturbed soils, tolerant to drought and of high added value in parallel with the development of agroforestry and valorization of organic waste, taking actions to protect local biodiversity and rehabilitate the areas that have undergone transformation. In addition, all mining companies have to run the so-called environmental monitoring.

2.5. European directives

Companies are increasingly required to disclose non-financial information to investors, so a set of guidelines has been developed to improve the standardization of environmental, social, and corporate governance (ESG) disclosure. In terms of (non-financial) reporting obligations, Directive 2014/95/EU covers the current requirements, but there have been a few recent regulatory developments. Among the most significant are the international initiative TCFD (Task Force on Climate-Related Financial Disclosures), as well as the CSRD (Corporate Sustainability Reporting Directive) package accompanied by ESRS (European Sustainability Reporting Standards) and Taxonomy system (Sustainable Finance Disclosure Regulation) SFDR. As a result of its adoption by Member States and implementation into national law, the CSRD recently replaced the existing NFRD (Woźniak et al., 2022).

2.6. Monitoring

The term monitoring describes a task area that involves the systematic monitoring of processes, procedures, behaviour and condition. Examples of this are environmental monitoring, which might include water, soil or air monitoring.

Any mining activity, from exploration to mining and reclamation, as well as infrastructure projects associated with mining, have an inevitable impact on ecosystems. To control and minimize the influence, it's critical to perform constant monitoring. Observation of land cover throughout the years helps notice the temporal, sometimes abnormal changes.

Monitoring the study area can be carried out in various ways. Depending on what needs to be documented and measured, field studies might be performed. Water or soil samples can be taken and later analyzed in laboratory conditions. Remedial measures such as fertilizers are selected and based on those studies.

2.6.1. Remote Sensing

In addition to ground-based monitoring, remote sensing and multispectral images play an important role in environmental monitoring. The use of GIS-supported analytical methods in assessing mining impacts has also been highlighted by Lechner et al., 2019.

The use of remote sensing techniques and geographic information systems has clearly shown advantages over standard laboratory measurements and field monitoring for assessing long- and short-term landscape dynamics. In large areas, where ground levelling and soil sampling are time-consuming, expensive, and labour-intensive. Remote Sensing and Geographic Information System provide prompt and efficient information about geological changes, the environment, and subsidence. Using these techniques, it is also possible to identify changes in the productivity and cover of vegetation, as well as flood dynamics, based on land-use and landcover maps. As a result of multispectral satellite images processing, it is possible to detect changes in landscapes that are both gradual and sudden (Padmanaban et al., 2017).

The application of RS and GIS in monitoring mining impacts on landscapes and the environment and associated geological changes and vegetation productivity is unfortunately limited. In some cases, remote monitoring of rehabilitated lands can be very challenging or impossible due to the land's inherently heterogeneous character. The rehabilitated land is usually created from patches of different vegetation in various development stages with specific soils. Landforms, slopes and topography, can vary greatly in a small area (McKenna et al., 2020). The quality and resolution of the spectral band might also cause a problem in the scientific description of the data.

RS derives data, which are later processed and analysed using GIS tools. It is a trivial and trending approach that enables analysis of large areas in a relatively short time. It's inexpensive because of open-access satellite missions and software.

Photogrammetry, as a technology that analyses photographs and enables geodetic measurements of distances, areas, or volume, can also be used as a tool to determine the extent of mining damage. It's important to carry out geodetic measurements regardless of whether the mine is active or closed down. These measurements usually consist of site surveys and levelling. Terrestrial laser scanning (LiDAR) is one of the most trending methods of land mapping in the modern world and has developed greatly. In this way, it is possible to determine horizontal displacements, subsidence, and deformations.

2.6.2. Satellite missions

Landsat 1 became the first earth-observing satellite explicitly designed to study planet Earth. It contributed invaluable data and launched a revolution in remote sensing technology. The aim is to constantly observe the entire planet and help in various research by expanding knowledge about remote sensing (*Landsat 1 | U.S. Geological Survey*, n.d.).

The SPOT series (French for "Satellite pour l'Observation de la Terre") has been providing high-resolution, wide-area optical images since 1986. Designed by France's National Center for Space Research (CNES), the five satellites were launched between 1986 and 2015 and their detailed discovery of the Earth's surface, have led to new applications in mapping, vegetation monitoring, land use and land cover and localizing the effects of natural disasters.

Sentinel-2's goal is to monitor land, and the mission will consist of two pole-orbiting satellites providing high-resolution optical images. Vegetation, soil and coastal areas are among the targets for monitoring. The first Sentinel-2 satellite was launched in June 2015.

The type of information collected varies depending on the needs and purpose of each mission. Not all data are seen as useful for every analysis. Some of them have characteristics that are deficient in some studies. For that reason, before collecting the data, proper criteria have to be defined. A possible set of criteria might be:

- temporal resolution (revisit time),
- spatial resolution,
- spectral resolution,
- open access data,
- cloud cover,
- swath width (Pawlik et al., 2021).

Table 1 contains a summary of chosen satellite missions and sensors that were reviewed for this study, presenting mentioned criteria.

Table 1. Comparison of satellite missions

Mission	Launch date	Swath width [km]	Spatial resolution [m] / Sensors ¹	Revisit time [days]	Spectral resolution
Landsat 1	July 23, 1972 – Jan. 6, 1978	185	RBV: 80, MSS: 80 (NIR)	18	4 bands
Landsat 2	Jan. 22, 1975 – Feb. 25, 1982	170/185	RBV: 80, MSS: 80 (NIR)	18	4 bands
Landsat 3	March 5, 1978 – Sep. 7, 1983	180	RBV: 40, MSS: 80 (NIR)	18	4 bands
Landsat 4	July 16, 1982 – June 15, 2001	185	MSS: 30 (80), 30/120 (TIR), TM: 30	16	7 bands
Landsat 5	March 1, 1984 – June 5, 2013	185	MSS: 30 (80), 30/120 (TIR), TM: 30	16	7 bands
Landsat 7	Apr. 15, 1999 -	185	ETM+: 30, 15 (PAN), 30/60 (TIR)	16	8 bands
Landsat 8	Feb. 11, 2013	185	OLI: 15 (PAN), 30 (MS), TIRS: 100	16	11 bands
Landsat 9 ²	Sep. 27, 2021 -	185	OLI: 15 (PAN), 30 (MS), TIRS: 100	16	11 bands
MODIS ³	Dec. 18, 1999 -	2330	250 (VNIR), 500 (VNIR, SWIR), 1000 (TIR)	2	35 bands
ASTER ⁴	Dec. 18, 1999 -	60	15 (VNIR), 60 (SWIR), 90 (TIR)	16	14 bands
DESI ⁵	June 29, 2018 -	30	30	3-5	235 bands
Sentinel-2 ⁶	June 23, 2015 -	290	10 (VNIR), 20 (VNIR, SWIR), 60 (CAVIS)	5	13 bands
GeoEye-1 ⁷	Sep. 6, 2008 -	15.2	0.41 (PAN), 1.64 (MS)	1.7 - 4.6	5 bands

¹ The abbreviations used in the table refer to products obtained from different spectral channels: RBV - Return Beam Vidicon, MSS - Multispectral Scanner, TM - Thematic Mapper, ETM+ - Enhanced Thematic Mapper Plus, OLI - Operational Land Imager, TIRS - Thermal Infrared Sensor, CAVIS - Clouds, Aerosols, Vapours, Ice and Snow, LISS-3 (LISS-4) - Linear Imaging Self-Scanning Sensor, AWiFS - Advanced Wide Field Sensor

² Landsat missions (Landsat 9 | Landsat Science, n.d.; Landsat Satellite Missions | U.S. Geological Survey, n.d.; Satellites | Landsat Science, n.d.)

³ MODIS (*MODIS Web*, n.d.)

⁴ ASTER (*LP DAAC - ASTER Overview*, n.d.)

⁵ DESIS (*DLR - Earth Observation Center - DESIS*, n.d.; Krutz et al., 2019)

⁶ Sentinel-2 (*ESA - The Sentinel Missions*, n.d.)

⁷ GeoEye-1 (*GeoEye-1 - Earth Online*, n.d.)

Mission	Launch date	Swath width [km]	Spatial resolution [m] / Sensors ¹	Revisit time [days]	Spectral resolution
SPOT 1	Feb. 22, 1986 – Nov. 2003	60	10 (PAN), 20 (MS)	2 - 3	4 bands
SPOT 2	Jan 22, 1990 - July 2009	60	10 (PAN), 20 (MS)	2 - 3	4 bands
SPOT 3	Sep. 26, 1993 – Nov. 1996	60	10 (PAN), 20 (MS)	2 - 3	4 bands
SPOT 4	March 24, 1998 – June 2013	60	10 (PAN), 20 (MS)	5	5 bands
SPOT 5	May 4, 2002 - March 2015	60	5/2,5 (PAN), 10 (MS), 20 (SWIR)	2 - 3	5 bands
SPOT 6	Sep. 9, 2012 -	60	1.5 (PAN), 6 (MS)	1 - 3	5 bands
SPOT 7 ⁸	June 30, 2014 -	60	1.5 (PAN), 6 (MS)	1 - 3	5 bands
WorldView-2	Oct. 8, 2009 -	16.4	0.46 (PAN), 1.8 (MS)	1.1 – 3.7	9 bands
WorldView-3 ⁹	Aug. 13, 2014 -	13.1	0.31 – 0.34 (PAN), 1.24 – 1.38 (VNIR), 3.70 - 4.10 (SWIR), 30 (CAVIS)	1 – 4.5	29 bands
QuickBird2 ¹⁰	Oct. 18, 2001 – Jan. 27, 2015	16,5	0,61 – 0,72 (PAN); 2,4 – 2,6 (MS)	1,5 – 2,8	5 bands
IRS-1C IRS -1D	Dec. 28, 1995 – Sep. 21, 2007 Sep. 29, 1997 – 2010	PAN: 70; LISS-III: 142, 148; WiFS: 810	PAN: ≤10, 5,6; LISS-III: 23,5 (VNIR), 70,5 (SWIR); WiFS: 188	24	5 bands
IRS-R2 ¹¹	April 20, 2011 -	LISS-4: 23.9, 70; LISS-3: 141; AWiFS: 740	LISS-4: ≤5.8; LISS-3: 23.5; AWiFS: 56, 70	24	4 bands

⁸ SPOT (Satellite Pour l'Observation de la Terre) missions (*SPOT - Earth Online*, n.d.)

⁹ WorldView Missions (*WorldView Series - Earth Online*, n.d.)

¹⁰ QuickBird-2 (*QuickBird-2 - Earth Online*, n.d.)

¹¹ IRS (Indian Remote Sensing) missions (*IRS-1C - Earth Online*, n.d.; *IRS-1D - Earth Online*, n.d.; *IRS-R2 (ResourceSat-2) - Earth Online*, n.d.)

The temporal resolution depends on the location of the sensor in relation to the target at the moment data is collected. It is described as nadir or off-nadir imagery with a given angular value. Another factor that impacts the revisit time is the swath width. The larger the area covered in each swath, the shorter the revisit time (Dwivedi, 2017).

Archived imagery from Landsat dates back to 1972. The sensor is one of the most commonly used for mapping vegetation (Xie et al., 2008). By combining Landsat 8 with Landsat 7 and the newly launched Landsat 9, Landsat 8's temporal resolution can be increased (*Landsat 9 | Landsat Science*, n.d.), (*What Are the Band Designations for the Landsat Satellites? | U.S. Geological Survey*, n.d.), (*Landsat Missions | U.S. Geological Survey*, n.d.).

Several competitive products have been developed from the ESA Sentinel program. The main advantage is the higher number of spectral bands and better spatial resolution (Table 2). In addition, the temporal resolution is 5 days (*ESA - The Sentinel Missions*, n.d.).

Missions such as Landsat or Sentinel distribute data free of charge, while some missions are commercial, so data must be bought. A discussion of that issue was conducted by (Radočaj et al., 2020). In recent years, attention has been drawn to the increase in applications of open data missions. It was the first Sentinel satellite launched in 2014 that played a critical role in this process. Additionally, as of 2 April 2016, the entire catalogue of ASTER image data became publicly available online at no cost (*Advanced Spaceborne Thermal Emission and Reflection Radiometer - Wikipedia*, n.d.).

ASTER and IRS series imagery have low temporal resolution, which means it is characterized by a long revisit period. Unlike the MODIS satellite, which provides an image every two days. Unfortunately, its weak point is that it presents a very low spatial resolution, which is unable to recognize minor changes (*MODIS Web*, n.d.), (*Moderate Resolution Imaging Spectroradiometer (MODIS) - LAADS DAAC*, n.d.). DESIS is a hyperspectral instrument located at the ISS. It is a type of mission, that works on request. For scientific purposes, there is a possibility to obtain DESIS imagery without charge. Unfortunately, the data is usually very limited, and for this study, there were only few images available (*DLR - Earth Observation Center - DESIS*, n.d.).

The WorldView series, GeoEye-1 and QuickBird2 satellites, like DESIS, also work on demand. These programs provide images with very high spatial resolution. Compared to other satellite data, monitoring relatively small areas would be possible with it. As a consequence, high-resolution data are stored in large files and need high computing power. The WorldView-1 is a panchromatic-only instrument which produces black-and-white imagery, that's why it wasn't taken into account. WorldView-4 also wasn't included in the compilation because it was launched in 2016 and ended in 2019 due to a failure (*WorldView-4 - Earth Online*, n.d.). The latest SPOT missions are other high-resolution commercial missions operating on request.

The sensors listed in Table 1 gathered multispectral and hyperspectral data (DESI). Especially for vegetation studies, it's crucial to select space missions that carry multispectral scanners (MSS). Not all space missions are equipped with appropriate sensors for research on vegetation indices. Spectral bands of space missions that met the required criteria are presented in Table 2.

Table 2. Characteristics of spectral bands and spatial resolution of satellite missions

Satellite mission	Sentinel 2			Landsat 8			Landsat 7			Landsat 4, 5		
Band 1	0,443	coastal aerosol	60	0.43-0.45	coastal aerosol	30	0.45-0.52	blue	30	0.45-0.52	blue	30
Band 2	0,490	blue	10	0.45-0.51	blue	30	0.52-0.60	green	30	0.52-0.60	green	30
Band 3	0,560	green	10	0.53-0.59	green	30	0.63-0.69	red	30	0.63-0.69	red	30
Band 4	0,665	red	10	0.64-0.67	red	30	0.77-0.90	NIR	30	0.77-0.90	NIR	30
Band 5	0,705	VRE	20	0.85-0.88	NIR	30	1.55-1.75	SWIR	30	1.55-1.75	SWIR	30
Band 6	0,740	VRE	20	1.57-1.65	SWIR	30	10.40-12.50	TIR	60 (30)	10.40-12.50	TIR	120 (30)
Band 7	0,783	VRE	20	2.11-2.29	SWIR	30	2.09-2.35	SWIR	30	2.09-2.35	SWIR	30
Band 8	0,842	NIR	10	0.50-0.68	PAN	15	0.52-0.90	PAN	15			
Band 8a	0,865	VRE	20									
Band 9	0,945	Water vapour	60	1.36-1.38	Cirrus	30						
Band 10	1,375	SWIR-Cirrus	60	10.60-11.19	TIRS 1	100						
Band 11	1,610	SWIR	20	11.50-12.51	TIRS 2	100						
Band 12	2,190	SWIR	20									
	wavelength (µm)		resolution (m)	wavelength (µm)		resolution (m)	wavelength (µm)		resolution (m)	wavelength (µm)		resolution (m)

Table 1, as well as Table 2, do not show data for Sentinel 1, Sentinel 3 and Sentinel 5P, as they are used in other areas: Sentinel 1- radar imaging mission for land and ocean services, observing Earth movements, Sentinel 3 –observation of sea, supports ocean forecasting systems, as well as environmental and climate monitoring and Sentinel 5P – in the study of the composition of the Earth’s atmosphere, providing timely data on a multitude of trace gases and aerosols affecting air quality and climate (Pawlik et al., 2021).

For vegetation observations, the Landsat 7, Landsat 8 and Sentinel-2 data display the best fit of the spectral ranges in terms of spatial resolution and frequency. Consequently, in most studies, research in this area is based on data from Landsat 7, Landsat 8 and Sentinel-2 (Buczyńska, 2020). A better understanding of the individual spectral bands of satellites allows for the calculation of vegetation indices, which are crucial for the process of geomonitoring post-mining conditions.

Multispectral images are recorded by a sensor located on the satellite. Satellite sensors receive signals in different wavebands (Table 2). These spectral ranges are called channels. Figure 2 presents the reflectance of water, soil and vegetation in different wavelengths. The wavelengths are presented for Landsat TM channels: 1 (0.45-0.52 μm), 2 (0.52-0.60 μm), 3 (0.63-0.69 μm), 4 (0.76-0.90 μm), 5 (1.55-1.75 μm) and 7 (2.08-2.35 μm). The spectral signature for green vegetation is very characteristic. In growing plants chlorophyll absorbs visible (blue and red) light to be used in photosynthesis, while near-infrared light is reflected effectively. The reflection from vegetation in the near-infrared and in the visual range of the spectrum varies considerably. The spectral signature of soils exhibits an increasing trend. Reflectance grows with increasing wavelength (*Classification Algorithms and Methods*, n.d.).

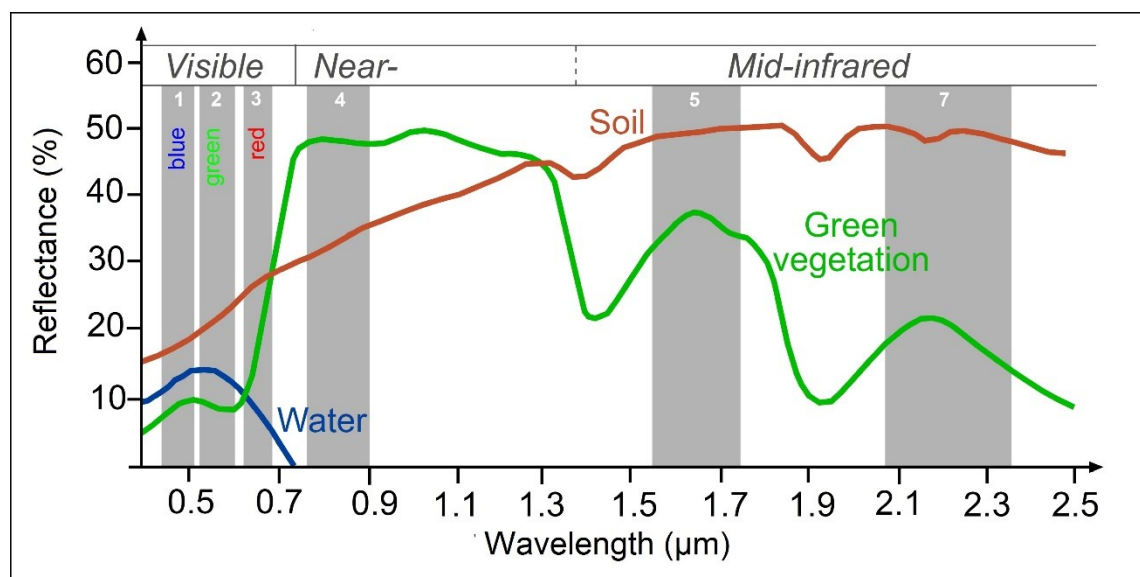


Figure 2. Reflectance of water, soil and vegetation in different wavelengths and Landsat TM channels (*Classification Algorithms and Methods*, n.d.)

2.6.3. Future satellite missions

Currently, there are several satellite missions planned to launch in the upcoming years. One of them, the FLuorescence EXplorer (FLEX) mission, will provide global maps of vegetation fluorescence that can reflect photosynthetic activity and plant health and stress, to do that it will be equipped with a high-resolution Fluorescence Imaging Spectrometer.

It will be the first satellite capable of measuring photosynthetic activity (*FLEX - Earth Online*, n.d.).

Next planned mission, Biomass, will provide crucial information about the state of our forests and how they are changing. The data will be used to further our knowledge of the role forests play in the carbon cycle. Furthermore, biomass will support UN treaties aiming to reduce deforestation and forest degradation emissions (*Biomass - Earth Online*, n.d.). For the first time from space, the satellite will carry a P-band Synthetic Aperture Radar (SAR) instrument to determine the amount of biomass and carbon stored in forests.

2.7. Environmental monitoring

2.7.1. Environmental indices

Acquiring data in many spectral ranges was the beginning to the creation of a new tool for assessing the components of the natural environment, which are environmental indices. To date, many indices have been developed for, among others, the assessment of the condition of vegetation cover and soils, estimation of water content in the environment, but also geological and landscape analyses (Buczyńska, 2020).

2.7.2. Monitoring of surface mining

Mining and subsequent restoration of the area manifest as sudden changes in vegetation cover. The vegetation happens to be severely damaged, especially during surface mining. Activities, such as soil reconstruction and planting trees, performed after completion of mining works, aim to achieve land and ecological restoration in opencast mines. As shown in Figure 3, the trajectory of the vegetation index can reflect the dynamic process of environmental impacts resulting from disturbances and recovery of vegetation. In terms of duration and magnitude, they indicate how long the event lasted and how much the vegetation index changed. It depends on the background environmental conditions, the spatial distribution pattern, and the mining development process (Liu et al., 2022).

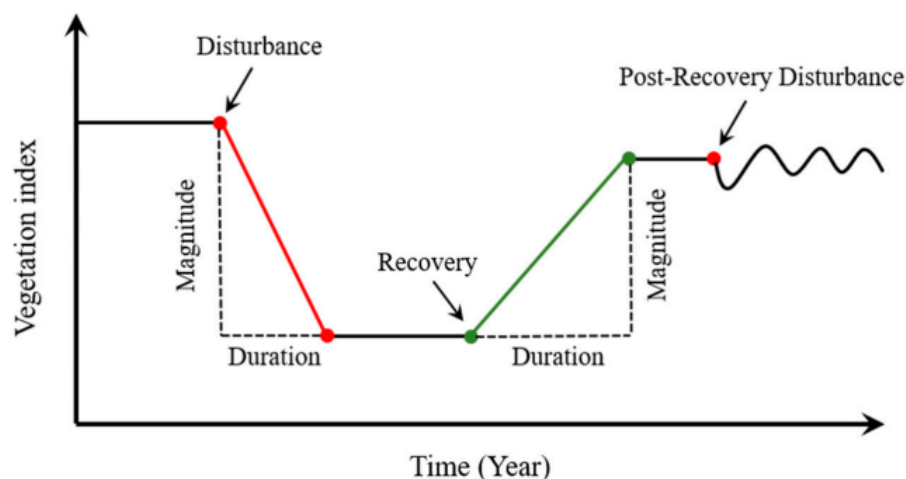


Figure 3. Schematic diagram of the vegetation index trajectory over time at a mine site (Liu et al., 2022)

2.7.3. Spectral indexes

Spectral indexes in post-mining refer to the use of spectral analysis techniques to monitor and assess the environmental impacts of mining activities on the landscape. These techniques involve analyzing the reflected light in different wavelength bands of remotely sensed images to identify changes in vegetation, soil, water quality, and other indexes of

environmental health. By measuring the reflected light in different bands, a spectral index can be created which can be used to map the changes in the environment over time. Spectral indexes are a useful tool for post-mining land reclamation and monitoring, as they can provide valuable information about the recovery of the ecosystem and any remaining impacts of mining activities. These indexes also can be used to detect early signs of degradation and track the effectiveness of reclamation efforts over time.

The purpose of this part of the work is to present a wide spectrum of possible applications of the environmental indexes created so far and indicate the most frequently chosen indexes. It's meant to summarize the research conducted in post-mining areas concerning the application of multispectral imaging to analyze changes in the elements of the natural environment. Selected indexes were presented and characterized in Table 3.

Many indexes have been developed that are used to analyze the state of elements in the natural environment. Therefore, there is a great deal of literature review available on the subject. These include, for example, the publication by (Pawlik et al., 2021), in which authors reviewed 42 vegetation indexes and their modified versions, and assessed their usefulness for geomonitoring of post-mining landscapes. It shared the definition of the vegetation index by (Jackson et al., 1983): "An ideal vegetation index would be highly sensitive to vegetation, insensitive to soil background changes, and only slightly influenced by atmospheric path radiance". Indexes presented in the study were divided into four groups. The first of these should be defined as basic, based on as few spectral channels as possible. These include e.g., NDVI, AVI, EVI, GNDVI. The second group are the indices based on the "soil line". These include e.g., SAVI1, SAVI2, TSAVI, MSAVI. The third group are indices, which take into account the influence of the atmosphere: ARVI, VARI. The fourth group consists of indices that study the chlorophyll content in vegetation e.g., CARI, MCARI, TCI (Pawlik et al., 2021).

In the publication by (Buczyńska, 2020) the following division of indexes determined on the basis of multispectral imagery was adopted:

- vegetation indexes - based on the characteristics of the reflection coefficient of the vegetation cover, it is possible to determine its condition, temperature, chlorophyll and carbohydrate content, the type of plants forming it and many other properties (Xue & Su, 2017),
- indexes determining the water content in the soil or vegetation,
- geological indexes to identify different types of rocks and minerals,
- indexes designed to detect areas that have been damaged by fires.

(Buczyńska, 2020) analyzed 20 publications focusing on the use of spectral indexes for post-mining areas. The results of the analysis of publications indicate that the scientific community in researching the natural environment in post-mining areas concentrates primarily on the analysis of the condition of the flora, the water content in the soil and plant cover, as well as the detection of areas where sedimentation of a certain type of minerals has occurred. Therefore, the review of the literature was narrowed down to vegetation, geological and water indexes. The subject of research on the use of vegetation indexes in the areas of mining extraction or those where mining activities have been discontinued is extremely wide. For the vegetation indices, the most frequently discussed topic was the monitoring of the reclamation process consisting of the analysis of spatio-temporal changes in the range of vegetation cover and its condition.

In the review prepared by (McKenna et al., 2020) the research for papers associated with spectral indexes was limited to years 1970-2019. The fifty years were chosen to adequately capture the beginning of earth observation through to the current era, and thus provide insight into the progress of rehabilitation assessments from relatively coarse resolution satellites to modern, high spatial and temporal sensors. 99 papers were analysed based on many features such as year of publication, place, types of ore and mine, type of sensor or spectral indexes. Landsat sensors were the dominant choice of sensor in 50% of studies over the 50-year period, but in the last decade, multiple earth observation and drone-based sensors across a diverse range of study locations contributed to our increased understanding of vegetation development post-mining. Thus, most of the studies (67%) were published from 2010-2019. In 2017, 2018, and 2019 drones were used in 25% of studies, aerial hyperspectral in 8%, aerial optical in 4%, and high-resolution earth observation Satellite Pour l'Observation de la Terre (SPOT) in 5% and WorldView in 3% of studies (McKenna et al., 2020). Remote sensing studies were mostly conducted on coal mines (62%), followed by metalliferous mines (17%) and quarries (5%). The study (McKenna et al., 2020) shows that out of 99 researched papers, NDVI was the most common index used, with 44 studies using this index. The next commonly applied index was SAVI with 7% of studies. EVI, NMDI and SR were used in 6 (6%) studies.

Currently, the Sentinel-2 images allow the use of about 250 unique vegetation indexes, which can find application in environmental monitoring (*IDB - Show Indices for Selected Sensor*, n.d.). Most vegetation indices have the same main purpose. However, each is specific in terms of emphasizing certain properties of vegetation or reducing noise due to the reflectivity of bare soil. Although the NDVI is the world's most widely applied vegetation index for a wide range of applications in monitoring vegetation properties (de Jong et al., 2011), it suffers from the limitation of low sensitivity to small differences in the case of high content of chlorophyll and biomass, the so-called saturation effect (Schaefer et al., 2016). The NDRE offers an alternative due to the enhanced sensitivity of the red coastal strip to these vegetation properties (Eitel et al., 2010). Soil adjusted vegetation index (SAVI) uses a correction factor to reduce the impact of bare soil reflection. And in the case of EVI, the blue band is applied to reduce the impact of atmospheric effects during remote sensing (Jiang et al., 2008). The secondary purpose of vegetation indices is to isolate areas under vegetation from soils and artificial land covers due to their sensitivity to chlorophyll content. The Modified Normalized Differential Water Index (MNDWI) is used to supplement vegetation indices when monitoring vegetation because it is sensitive to the water content in vegetation as well as in soil. It is a modified version of the Normalized Differential Water Index (NDWI). It was improved by using the green band instead of the near-infrared spectral band to reduce noise in the detection of soil and vegetation water content (Xu, 2006). By achieving maximum values for water surfaces, MNDWI is also used in land cover mapping (Radočaj et al., 2020).

2.7.4. Recent publications on spectral indexes application

Reclaimed areas located close to the mine, where they may be contaminated, e.g., by dust, related to active mining, require additional monitoring. Sedimentation or dust on the surface of the vegetation cover changes the reflection coefficient in individual spectral channels. This property was used in the work of (Ma et al., 2017), in which the authors, using 8 vegetation indexes (SR, NDVI, SAVI, TSAVI, PVI, NLI, MSR and $TC_{\text{greenness}}$), identified the amount and spatial distribution of dust deposited on leaves. Based on the laboratory tests and satellite images, the spectral responses of vegetation were analyzed depending on the mass of the accumulated dust. The obtained results indicate that with

the increase in the amount of dust, the reflection coefficient in the red channel increases, while it decreases in the near-infrared channel. The studies also showed that the vegetation indices are linearly or logarithmically related to the mass of dust deposited on the leaf surface. Finally, the authors concluded that the SAVI, TSAVI, PVI, NI and MSR indexes are not suitable for the study of tall and multi-species vegetation.

In addition to the use of vegetation indexes, spectral geological indexes can be used to detect deposits of mining origin and identify areas where sedimentation of a specific rock formation or minerals has occurred. Water reservoirs created as a result of mining activities are characterized by a significant content of heavy metals. Therefore, the spectral curves resulting from the reflection of the electromagnetic wave from the surface of the contaminated tank will differ from the curves recorded for tanks that do not contain heavy metals. Research aimed at identifying post-mining reservoirs among existing bodies of water was undertaken by (Mukherjee et al., 2018). The authors, using the images of the Landsat 8 satellite, used the NDWI, Bare Soil Index (BI) and Clay Minerals Ratio. The NDWI index enabled the detection of water reservoirs among other forms of land use. Then the BI index, whose task was to eliminate the misinterpretation of the exposed soil as a body of water. The implementation of the goal set by the authors was made possible by the Clay Minerals Ratio index. In their next publication (Mukherjee et al., 2019), the authors continued this research, showing that the Iron Oxide Ratio allows for higher accuracy in identifying post-mining reservoirs than the Clay Minerals Ratio.

Remote sensing showed potential for soil organic carbon (SOC) mapping in exposed croplands. Unfortunately, some disturbing factors interfere with SOC prediction, such as photosynthetic and nonphotosynthetic active vegetation, variation in soil moisture or surface roughness. There are methods to stabilize soil reflectance by building image composites. They tend to minimize disturbing effects by using sets of criteria. The study by (Dvorakova et al., 2021) deals with using satellite imagery from the Sentinel-2 satellite to create a composite image to predict soil organic carbon levels in exposed soil. Authors selected all S-2 cloud-free images covering the Belgian Loam Belt from January 2019 to December 2020 and later built nine exposed soil composites based on four sets of criteria: lowest Normalized Burn Ratio (NBR2), (NDVI) and the 'greening-up' period of a crop. The 'greening-up' period was selected based on the NDVI timeline, where 'greening-up' is considered as the last date of acquisition where the soil is exposed ($NDVI < 0.25$) before the crop develops ($NDVI > 0.25$). The 'greening-up' method combined with a strict NBR2 threshold allows the selection of the purest exposed soil pixels suitable for SOC prediction. In two years, this method covered 62% of the total cropland area, compared with 95% if only the NDVI threshold was used.

Due to the faster development of society and the increased demand for raw materials, there is a need to explore the Earth to identify new, potential deposits of mineral deposits. Geological indexes developed based on high-resolution multi-spectral imaging provide an opportunity to achieve this goal remotely and economically. An example of an analysis of this type is the research conducted in the Bau mining area on the island of Borneo (Pour & Hashim, 2014). The authors, based on indices such as: Clay minerals ratio, ferric iron oxide index or ferrous iron oxide index, identified areas hydrothermally changed as a result of gold mineralization.

The use of spectral indexes determining water content in post-mining areas has been presented in the paper from (Yu et al., 2016). The authors analyzed changes in the spatial range of rivers in the years 2002-2014 located near the Xinjiang hard coal mine. The authors based their research on two spectral indices: MNDWI and Blue and Near Infrared

Band based Water Index (BNWI) developed based on Landsat 5 and 8 satellite images. The obtained results confirmed that the analyzed watercourses decreased in size. The overall accuracy of the method used in the study was over 90%.

Publication (Gadal et al., 2021) describes a study that uses Sentinel 2 satellite images to analyze the soil degradation risk on the Cameroonian shores of Lake Chad and its surrounding area. The study combines spectral indices and statistical analysis to develop a new method of analyzing soil degradation. Four vegetation indices, such as greenery index and water stress index, and nine soil indices, such as moisture, luminosity or organic matter content, were selected and calculated to characterize vegetation cover and bare soil condition. All these indices were aggregated to produce one image and then regressed by individual indices to retrieve correlation and determination coefficients. Principle Component Analysis and factorial analysis were applied to all spectral indices to summarize information, obtain factorial coordinates, and detect positive/negative correlations. The first factor contained soil information, the second factor contained vegetation information. The final equation of the model was obtained by weighting each index with both its coefficient of determination and factorials coordinates. This result generated figures cartography of five classes of soils potentially exposed to the risk of soil degradation. Five levels of exposition risk were obtained from the "Lower" level to the "Higher".

In (Madasa et al., 2021) study, remote sensing was used to quantify land-use/cover changes in the Welkom – Virginia Goldfields. The aim was to analyse Landsat images with a 5-year interval from 1988 to 2018 using geospatial indices: Global Environmental Monitoring Index (GEMI), the Normalized Difference Built-up Index (NDBI), the NDVI, the Normalized Difference Soil Index (NDSI) and the NDWI to distinguish different types of land cover. To classify the images, the maximum likelihood method was implemented for supervised classification. Various land-use changes were found, with fluctuating values for each index, ranging from 88% to 96% for the overall accuracy of the classified images. Thus, these indexes are reliable for tracking changes in land use in mining areas over a wide area.

This chapter was devoted to the general topic of the use of spectral indices in determining the state of the environment or using them for land classification. The next chapter focuses exclusively on methods of monitoring in post-mining landscapes.

Table 3. Selected vegetation and water indices found in the literature

Index	Abb.	Formula ¹²	Description	References
Vegetation Indices				
Normalised Difference Vegetation Index	NDVI	$= \frac{NIR - RED}{NIR + RED}$	Used to evaluate the chlorophyll activity of plants and also for monitoring the state of the vegetation cover. It has a limitation in the form of low sensitivity to minor differences in the case of high chlorophyll content and biomass, known as the saturation effect. Sensitive to atmospheric phenomena, light, and sand oil colour, leading to decreased accuracy.	(Karan et al., 2016) (Ma et al., 2017) (Tuominen et al., 2009) (Dvorakova et al., 2021) (Köhler, 2019)
Enhanced Vegetation Index	EVI1	$= G * \frac{NIR - RED}{NIR + C_1RED - C_2BLUE + L}$ G – gain factor, C1 – coefficient of aerosol resistance, C2 – coefficient of aerosol resistance, L – soil adjustment factor.	A blue band for the calculation of EVI1 is used to correct the effects of atmospheric factors and soil signals at the same time, especially in areas with dense crowns, EVI1 performs better in areas characterized by significant ‘woodiness’.	(Karan et al., 2016) (Buczyńska & Blachowski, 2021) (Liu & Huete, 1995) (A. Huete et al., 2002)
	EVI2	$= 2,5 * \frac{NIR - RED}{NIR + 2,4 * RED + L}$	The index is designed achieve similar values to EVI1, applied for instruments without a blue band. The role of the blue band in the EVI1 doesn’t provide additional biophysical information on vegetation properties.	(Jiang et al., 2008)
Soil Adjusted Vegetation Index	SAVI	$= \frac{NIR - RED}{NIR + RED + L} * (1 + L)$	This transformation is most appropriate for identifying soil-induced changes in vegetation indices. It minimalizes soil-brightness influences with constant L.	(Ma et al., 2017) (A. R. Huete, 1988) (Major et al., 1990) (Jiang et al., 2008)

¹² Coefficients used in formulas refer to spectral bands (NIR – near infrared, SWIR - shortwave infrared, MIR – mid infrared)

Index	Abb.	Formula ¹²	Description	References
Modified Soil Adjusted Vegetation Index	MSAVI2	$= \frac{2NIR + 1 - \sqrt{(2NIR + 1)^2 - 8(NIR - RED)}}{2}$	Describes vegetation density and reduces the effects of soil, in particular when the canopy is sparse, especially in arid and semi-arid environments. Used in the analysis of plant growth, desertification research, analysis of soil organic matter, drought monitoring and the analysis of soil erosion.	(Chen, 1996) (Qi et al., 1994) (Gadal et al., 2021)
Simple Ratio	SR	$= \frac{NIR}{RED}$	The index responds better to changes in biomass in later stages of growth. On the other hand, it is of little use to describe biomass with less than 50% vegetation cover, as it is sensitive to atmospheric effects.	(Ma et al., 2017) (Xue & Su, 2017) (Viña et al., 2011) (Erener, 2011)
Ratio Vegetation Index	RVI	$= \frac{RED}{NIR}$	Ratios are usually designed to highlight the target features as high-ratio Digital Numbers (DNs). RVI is also well-known as an effective technique for suppressing topographic shadows.	(Karan et al., 2016) (Bannari et al., 1995) (Richardson & Wiegand, 1977)
Green Normalized Difference Vegetation Index	GNDVI	$= \frac{NIR - GREEN}{NIR + GREEN}$	It is most often used to assess plant leaves' moisture content and nitrogen concentration according to multispectral data that do not have an extreme red channel. It is more sensitive to the presence of chlorophyll. It is used to assess depressed and ageing vegetation.	(Buczyńska & Blachowski, 2021) (Sanjerehei, 2014) (Gitelson et al., 1995)
Visible Atmospheric Resistant Index	VARI	$= \frac{GREEN - RED}{GREEN + RED - BLUE}$	It aims to emphasize vegetation in the visible part of the spectrum while softening differences in lighting and atmospheric effects.	(Gitelson et al., 2002)
Bare Soil Index	BSI (BI)	$= \frac{(SWIR1 + RED) - (NIR + BLUE)}{(SWIR1 + RED) + (NIR + BLUE)}$	Higher values of this index detect the bareness of a region. The bare soil map is removed from the water map for further processing.	(Mukherjee et al., 2018)

Index	Abb.	Formula ¹²	Description	References
Water Content Indices				
Normalized Difference Water Index	NDWI	$= \frac{GREEN - NIR}{GREEN + NIR}$ (McFeeters, 1996)	This index is designed to maximize the reflectance of water by using green wavelengths; minimize the low reflectance of NIR by water features; and take advantage of the high reflectance of NIR by vegetation and soil features. As a result, water features have positive values and are thus enhanced, while vegetation and soil usually have zero or negative values and are suppressed.	(Xu, 2006) (Yu et al., 2016) (McFeeters, 1996) (Acharya et al., 2018) (Mukherjee et al., 2018)
Normalised Differenced Moisture Index	NDMI (NDWI _{Gao} (Gao, 1996))	$= \frac{NIR - MIR}{NIR + MIR}$	NDMI, also described as NDWI _{Gao} , is correlated with the canopy water content. Thus, it is better for tracking changes in water stress and plant biomass.	(Xu, 2006) (Karan et al., 2016) (Wilson & Sader, 2002)
Modified Normalized Difference Water Index	MNDWI	$= \frac{GREEN - SWIR}{GREEN + SWIR}$	The contrast between water and built-up land will be considerably enlarged owing to increasing values of water feature and decreasing values of built-up land from positive down to negative. The greater enhancement of water will result in more accurate extraction of open water features as the built-up land, soil and vegetation all have negative values and thus are notably suppressed and even removed.	(Xu, 2006) (Yu et al., 2016) (Radočaj et al., 2020)
Blue and Near Infrared Band-based Water Index	BNWI	$= \frac{NIR - BLUE}{NIR + BLUE}$	Introduced to separate shadows and water pixels.	(Yu et al., 2016)
Moisture Stress Index	MSI	$= \frac{SWIR1}{NIR}$	Used to evaluate the spatial extent of less soil moisture, due to the higher level of evapotranspiration	(Gadal et al., 2021)

2.8. Reclamation monitoring methods in recent publications

This literature review provides an understanding of the topics related to this study. GIS and remote sensing have been used extensively in the literature to monitor landscapes that have been affected by mining. In most research studies, researchers concentrate on agricultural vegetation, since flora constitutes a valid indication of the current state of restoration of the land. Presented in Table 4 five example cases are focusing on monitoring post-mining landscapes. They were selected based on the year of publication, the type of monitored area, type of satellite data and the vegetation indexes used in the analysis. The presented case studies were used to understand the topic and to help develop the study.

Table 4. Summary of chosen case studies found in recent research publications.

Study	Study area	Satellite mission	Method	Indices
(Liu et al., 2022)	Inner Mongolia, China (1986-2020)	Landsat 5, 7, and 8	Vegetation trajectory Landtrendr algorithm	NDVI
(Kuzevic et al., 2022)	Rohožník-Konopiská and Sološnica-Hrabník deposit, Slovakia (1990-2021)	Landsat 5, 7, 8, Corine land cover (CLC)	Land Cover and Vegetation Coverage Changes	NDVI
(Buczyńska Blachowski, 2021)	& Babina lignite mine, Poland (1989-2019)	Landsat	Time series analysis, correlation, change detection	NDVI, EVI, RVI, NDMI
(Li et al., 2020)	Shengli coal mine, Inner Mongolia Autonomous Region, China	Landsat	Reclamation trajectory, Random Forest classification	NDII, MSAVI2
(Karan et al., 2016)	Jhartia coalfield, Damodar River Valley, India	Landsat	Support Vector Machines (SVM) classification, change detection	NDVI, RVI, EVI, NDMI

In a study by (Liu et al., 2022), long-term monitoring from 1986 to 2020 was implemented by the LandTrendr algorithm to reveal the ecological impacts of two concentrated and contiguous surface mining sites with different mining patterns and surrounding environments in Inner Mongolia, China. The LandTrendr algorithm is a suitable method

for monitoring vegetation dynamics, which includes both disturbance and recovery. The algorithm captures mining and restoration events at the mining sites by the point in time when the change in the spectral-temporal trajectory occurs. The study used archived Landsat TM/ETM+/OLI image data (Landsat 5, 7, and 8). Based on the NDVI characteristics of the study area, loss and increase of vegetation indicated disturbance and recovery respectively. Results showed that the application of the LandTrendr algorithm for surface mining site monitoring is appropriate, with an overall accuracy of around 75% for disturbance and recovery. The magnitude of recovery decreases first with increasing duration and then reaches the natural fluctuation state after 20 years of recovery. Therefore, surface mining sites in ecologically fragile areas are more suitable for long-term mining, and monitoring should extend more than 20 years after restoration.

The main objective of the paper by (Kuzevic et al., 2022) was the mapping of spatio-temporal changes in the landscape in connection with the extraction of minerals due to mining activities on the landscape. The study used Corine land cover (CLC) data and Landsat 5, 7, and 8 satellite images for selected years in the period 1990–2021. The study was specific to the presence of four mineral deposits (three of them are under active mining). The Rohožník-Konopiská deposit in Slovakia was abandoned and the area was subsequently reclaimed. NDVI was calculated for vegetation cover analysis, which was further combined with the forest spatial division units (FSDU) layer. Areas near the mine were selected for a detailed analysis of changes in vegetation. An average NDVI index value was calculated using the FSDU data and the Zonal statistics function for each plot. The results showed that for the two deposits Rohožník-Konopiská (inactive) and Sološnica-Hrabník (active), there have been changes indicating an improvement in the landscape condition by reclamation operations.

The purpose of the publication by (Buczyńska & Blachowski, 2021) was to present the changes in the condition of plant cover within the Pustków mining field of the closed lignite “Friendship of Nations - Babina Shaft” mine. The analysis was carried out from 1989 to 2019 based on NDVI, EVI and GNDVI spectral indices, developed using multispectral images of the Landsat TM/ETM+/OLI missions. The obtained results indicate a systematic improvement in flora conditions in the analysed region, but also an increase in green areas. Observations included overgrown shorelines at anthropogenic lakes and heaps, as well as a reservoir with a decreasing surface area due to vegetation succession. Additionally, local plant cover degradation was observed in Pustków's north-western area in 2016. According to the obtained results, continuous monitoring of the flora's health is necessary not only in the area of the analysed mine but also in other post-mining areas.

In some cases (Li et al., 2020), monitoring by remote sensing is enhanced by field surveying. The study examined the succession trajectory types of revegetation at three coal-waste dump sites with different reclamation methods to determine if revegetation had been restored to its pre-disturbance state. To this end, the authors proposed an analysis method that uses a machine learning method with a traditional method of statistical analysis using multi-time Landsat images and geodetic data. Landsat imagery was used in order to assess vegetation characteristics. MSAVI2 provided information on greening, while the Normalized Difference Infrared Index (NDII) described vegetation moisture and canopy water thickness. The study showed the time series remote sensing trajectory analysis and field investigation analysis were complementary to each other and could reflect the mining influence and reclamation effect more comprehensively and effectively.

The subject of monitoring the reclamation process consisting in the analysis of spatial-temporal changes in the range of the vegetation cover and its condition is addressed in the publication (Karan et al., 2016), in which the flora in the reclaimed block II of the Jharia coal mining area was analysed. By using Landsat 5 and 8 satellite images, three vegetation indexes (NDVI, EVI, RVI) and an index enabling the analysis of water content in vegetation (NDMI) were developed. The process allowed for the identification of land cover forms in the study area, along with an indication of their changes over the last 15 years. It also made it possible to assess the condition of the existing vegetation. The authors found a correlation between some of the indexes, particularly NDVI and EVI, as well as NDVI and NDMI.

2.9. Summary

A review of the literature presented in several chapters gives an insight into the scope of the study. Reclamation requires monitoring. Using GIS and RS monitoring of reclaimed post-mining landscapes can be accomplished. According to most publications, vegetation analysis is the most reliable measure of reclamation success. Additionally, multispectral imagery was reviewed as part of the literature review. Various satellite missions were characterised with the aim of selecting the most appropriate for this study.

Based on the characteristics of the spectral indexes, results of literature review and specification of the case study site presented in previous chapters Landsat satellite data and vegetation spectral indexes were selected and the methodology described in the next chapter.

3. Data requirement and methodology

The first step in processing satellite images for spectral indexes is to acquire the images. This can be done by using a variety of satellite platforms, such as Landsat, Sentinel, or MODIS, that were mentioned before, which collect images at different wavelengths of light. Once the images have been acquired, they must be pre-processed to remove any errors or distortions that may be present. This can include removing cloud cover, correcting for atmospheric effects, and removing sensor noise. Next, the images must be calibrated to ensure that they are accurately measuring the reflectance of the earth's surface. After the images are calibrated, the spectral indexes can be calculated. This is done by using mathematical algorithms that use the reflectance of different wavelengths of light to identify specific features on the earth's surface.

3.1. Data acquisition

This study focuses on imagery data from the Landsat 4, 5, 7 and 8 mission. Data was collected through the United States Geological Survey (USGS). The imagery can be downloaded directly through the web page (*EarthExplorer*, n.d.), but also using the Semi-Automatic Classification Plugin (SCP) which is a free open-source plugin for QGIS. Data must be selected by specifying the area of interest and time.

3.2. Processing

The aim of pre-processing is to correct the radiance differences caused by variations in solar illumination, atmospheric conditions, sensor performance and geometric distortions respectively. Another aim is to enhance the image data information by filtering or data fusion techniques (Nussbaum & Niemeyer, 2009). Not all data require pre-processing.

Some of the newest satellite images have already gone through the process of necessary corrections. Various image processed levels for Landsat are presented on Figure 4.

Landsat data are available within Collection 2 in two levels of processing, Level-1 and Level-2. Level-1 data are in the form of Digital Numbers ready for preprocessing in connection with the conversion to Top of Atmosphere (TOA) reflectance or radiance. The Landsat satellite imagery used in this study was downloaded from Collection 2 Level-2 already with surface reflectance values and no further atmospheric correction is required. The Level-2 images are directly usable for the spectral indexes calculation.

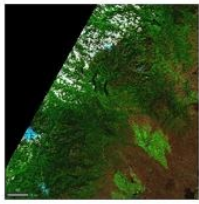
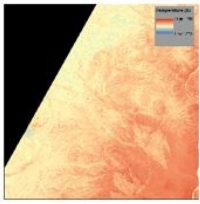
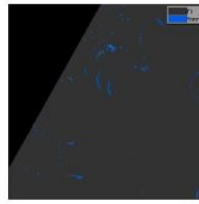
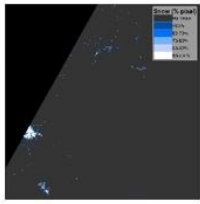

Landsat Level-2 Products		Landsat Level-3 Products		
Surface Reflectance	Provisional Surface Temperature	Dynamic Surface Water Extent	Fractional Snow Covered Area	Burned Area
Measures the fraction of incoming solar radiation that is reflected from Earth's surface to the Landsat sensor	Represents the temperature of the Earth's surface in Kelvin (K)	Describes the existence and condition of surface water	Indicates the percentage of a pixel covered by snow	Represents per pixel burn classification and burn probability
				

Figure 4. Landsat Level-2 and Level-3 Science Products (Landsat Level-2 and Level-3 Science Products | U.S. Geological Survey, *n.d.*)

Downloaded images have been checked for cloud disruption or shadows. The project's coordinate reference system was WGS 84/Zone 33N. Some of the downloaded data were assigned to Zone 32N. Reprojection of these images was performed using *Warp (reproject)* tool.

Build virtual raster tool was used to process the imagery. Bands used for calculating the indexes were added to build the multiband rasters. The images were limited by using a *Clip raster by mask layer* to reduce the size of data and speed up subsequent operations.

Calculation of the indices was executed for each scene in the dataset using the *Raster Calculator* tool. In the case of Landsat 4-5 and 7 imagery, the blue channel is marked as band 1, and the red channel is marked as band 3. Reflectance in NIR is stored in band 4 and SWIR is stored in band 5. For Landsat 8-9 the blue channel is marked as band 2, the red channel as band 4, reflectance in NIR is stored in band 5 and SWIR stored in band 6.

Statistics including mean value and standard deviation were derived using the *Zonal Statistics* tool for each scene.

3.3. Indexes

The targeted monitoring concept is based on spectral indexes based on a literature review and open source, tested on an example in Germany. The suitable indexes presented in Table 3 have been selected to monitor the changes in post-mining landscape, as a part of the workflow.

Various indexes of vegetation can be used to monitor the state of the environment. One of the most popular is the Normalized Difference Vegetation Index (Rouse J.~W. et al., 1974). The NDVI index is the most frequently used vegetation index in scientific research and in practice. The analysis of the NDVI value allows to distinguish vegetation from

other (artificial) types of land cover and determine the stage of development and condition of plants. NDVI allows you to define and visualize areas covered with vegetation on the map, as well as detect abnormal changes in the process of plant growth. Red and near-infrared (NIR) reflectance values are used to calculate the NDVI value. It is highly sensitive to aerosols and atmospheric phenomena, leading to decreased accuracy. There are also some limitations due to soil background brightness.

The calculation of the NDVI is as follows (1):

$$NDVI = \frac{NIR - Red}{NIR + Red} \quad (1)$$

NIR - reflectance in the near-infrared channel,

Red - reflectance in the red channel.

EVI1 performs better in areas characterized by significant 'woodiness', for which the land cover with NDVI may show irregularities (NDVI saturation occurs in areas characterized by high biomass). In addition, using the blue band EVI1 reduces the influences of the atmosphere and minimizes canopy background brightness (Pettorelli, 2013).

It is described by (2):

$$EVI1 = G * \frac{NIR - R}{NIR + C_1R - C_2B + L} \quad (2)$$

G – gain factor, by default set to 2.5,

C₁ – coefficient of aerosol resistance, set by default to 6,

C₂ – coefficient of aerosol resistance, set by default to 7.5,

L – soil adjustment factor, set by default to = 1 (Pawlik et al., 2021).

The relationship between red and blue reflectances is highly correlated. The blue band does not contribute much additional information about the land surface than the red band at the canopy level and when atmospheric effects are insignificant. By simply assuming the relationship, $Red = c * Blue$, the EVI1 equation (2) can be reduced to a 2-band EVI2 equation (3) using the L, C_1 , and C_2 values mentioned above (Jiang et al., 2008).

$$EVI2 = G * \frac{NIR - R}{NIR + (6 - 7,5/c) * R + 1000} \quad (3)$$

c - the ratio of red to blue reflectances.

EVI2 can also be expressed as a function of the ratio of red to blue reflectances, c . The mean absolute difference between EVI and EVI2 is minimum when $c = 2.08$, with the corresponding G equal to 2.5. The optimal c and G values render previous equation to be the same as (with scaling factor set to 1000) (4):

$$EVI2 = 2,5 * \frac{NIR - R}{NIR + (6 - 7,5/2,08) * R + 1000} = G * \frac{NIR - R}{NIR + 2,4 * R + 1000} \quad (4)$$

The NDVI value may be influenced by parameters such as soil colour and moisture, as well as vegetation density. In addition, with a dense vegetation cover, the NDVI index experiences a saturation of the reflection, i.e., with a large biomass, its further increase does not increase the value of the index. To minimize the effect of soil brightness, the SAVI (Soil Adjusted Vegetation Index; (A. R. Huete, 1988)) can be used to assess the condition of vegetation, which performs better than NDVI in areas with low vegetation

density. The SAVI index is calculated based on the same spectral ranges as the NDVI, but with an additional soil parameter L ranging from 0 (for very dense vegetation cover) to 1 (for very little vegetation cover), most often 0.5 (numerous modifications are also used SAVI with a function describing the value of L).

The formula for calculating the SAVI index (5):

$$SAVI = \frac{NIR - Red}{NIR + Red + L} * (1 + L) \quad (5)$$

NIR - reflectance in the near-infrared channel,

Red - reflectance in the red channel.

4. Input data

4.1. Satellite data

Landsat-5 Enhanced Thematic Mapper (ETM) and Landsat-8 Operational Land Imager (OLI)/Thermal Infra-Red Sensor (TIRS) and a few additional Landsat 7 data of 30 × 30 m spatial resolution were acquired for ten chosen years at four-year interval (1986, 1990, 1994, 1998, 2002, 2006, 2010, 2014, 2018 and 2022) and analysed to determine the change in the vegetation cover in the study area. The study focuses on months high in vegetation, that is June, July and August. Most of the acquired images had 0% cloud coverage and were downloaded from the United States Geological Survey (USGS) website (*EarthExplorer*, n.d.). Majority of the available images from Landsat 7 were omitted due to the failure of Landsat 7’s Scan Line Corrector on the 31st of May 2003. The Scan Line Corrector’s role was to compensate for the forward movement of the satellite as it orbits, and the failure means instead of mapping in straight lines, a zigzag ground track is followed. This causes parts of the edge of the image not to be mapped (*Five Landsat Quirks You Should Know | Pixalytics Ltd*, n.d.). Hence presenting the black stripe effect and resulting in a useless image.

The four-year interval was chosen to minimize the size of the data and better represent changes in the landscape. The selected years turned out to be the most suitable. After preliminary analyzes of satellite images and the selection of a five-year range, the years 1985, 2000 and 2005 showed a lack of data, due to cloud cover.

In the end, a total of 33 images were selected and downloaded. The dates and satellite missions of images used for this study have been presented in Table 5.

Table 5. Landsat images acquired from 1 June to 31 August in the years 1986-2022

1986			1990			1994			1998			2002			2006			2010			2014			2018			2022					
June	July	August	June	July	August	June	July	August	June	July	August	June	July	August	June	July	August	June	July	August	June	July	August	June	July	August	June	July	August			
31	7		2	21		23	8	17	10	20		11	13		6	8		10	3		7	8	15	17	2							
			3	28			17			27			22			17			19		14	23										
																					23											

Landsat 4-5
 Landsat 7
 Landsat 8

Lack of data for June and August in some years have resulted in exclusion of these months. According to the literature it is important to analyse vegetation spectral indexes acquired in the same phenological season, therefore data from the same month in the selected years were selected. Only 15 images presented on Table 5 with bold font, were chosen for processing and later analysis. These images will be processed and used in later analysis.

4.1. Study area

The area of interest is located in the Profen opencast mine in the south of Saxony-Anhalt in Germany (Figure 5). It stretches across the Profen Süd, Schwerzau and Domsen mining fields. It is operated by the Mitteldeutsche Braunkohlengesellschaft (MIBRAG) (Figure 6). Annual extraction reaches up to 5 to 6 million tons of raw brown coal (*Tagebau Profen* - MIBRAG MbH, n.d.).



Figure 5. Map showing the location of the Profen mine in Germany



Figure 6. Map of the Profen mine (Braunkohlengesellschaft mbH MIBRAG & Kappa GmbH, n.d.)

Modern opencast mining and rehabilitation are inseparable. Together with regional planning, municipalities, associations, authorities and citizens, MIBRAG plans and designs a versatile and ecologically valuable post-mining landscape (Braunkohlengesellschaft mbH MIBRAG & Kappa GmbH, n.d.).

Since there was mainly agricultural land before the Profen opencast mine, a large proportion of the dumping ground is also being prepared for agricultural use (Figure 7). For this purpose, the areas are cultivated in a fixed crop rotation over a period of seven years. This enriches and homogenizes the soil with organic substances. This helps build a stable soil structure. The recultivated mining areas also offer numerous animal and plant species new habitats and people opportunities for recreation (Braunkohlengesellschaft mbH MIBRAG & Kappa GmbH, n.d.).

This study focuses on post-mining landscapes reclaimed towards forestry. The detailed information regarding forest reclamation process was obtained from MIBRAG Company. Each site is treated differently. Before plantation of trees, a soil survey is carried out. Profen reclamation sites are usually very heterogeneous, with pH-values ranging from 2,5 to 8,0. The soil composition and nutrient contents might vary strongly.

The forestry reclamation generally starts with a ground cover (a mixture of clover species), while the soil survey is carried out. The clover cover prevents erosion and starts adding organic matter and nutrients to the soil. With the results from the soil survey lime is being added to the sites to adjust the pH-value. The lime is worked into the soil with a deep-tillage machine, which is attached to a tractor (this mixes the lime into the ground to about 1 m depth). Ideally, a year needs to pass for the lime to react in the soil and then another soil survey is carried out to make sure the desired effects have been reached.

After the soil melioration (“Grundmelioration”) and the adding of fertiliser, the site can be planted with forest trees. There are different approaches here, depending on the site and the soil quality, but usually a mixture of birches, alder, poplar, and oak is planted. The soil survey is very important in determining how the site is prepared and which tree species are planted.

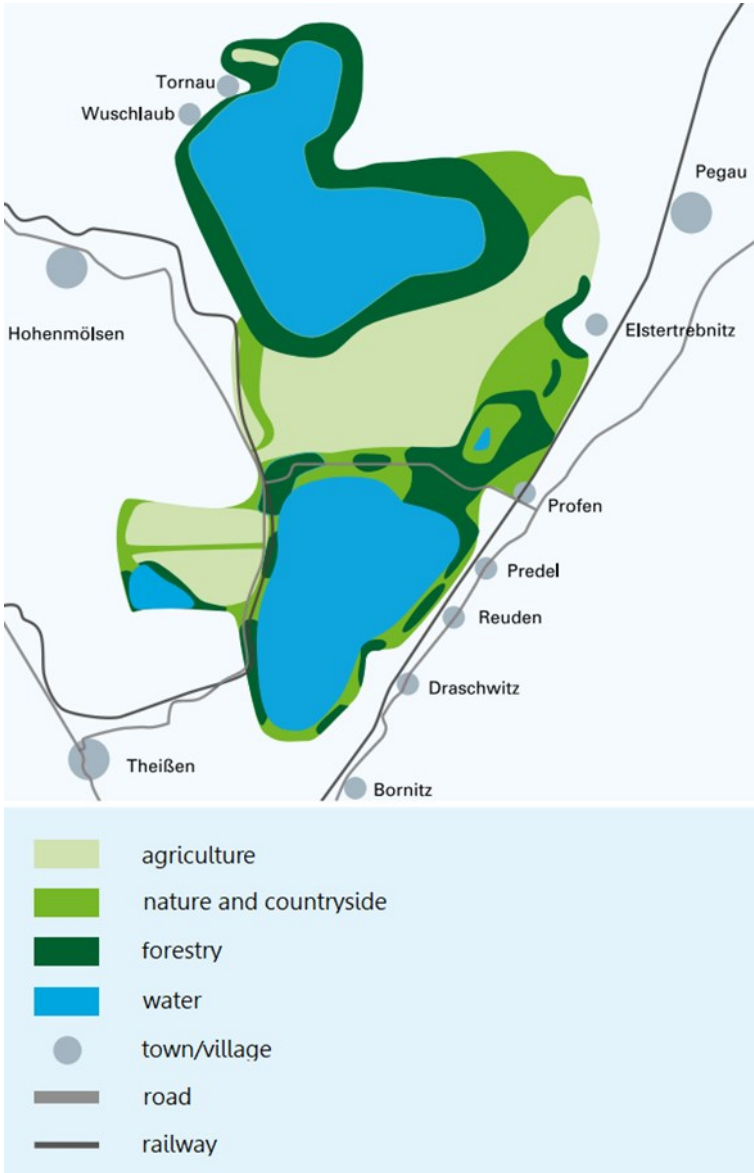


Figure 7. A vision of the post-mining landscape at The Profen mine (Braunkohlengesellschaft mbH MIBRAG & Kappa GmbH, n.d.)

4.2. Droughts in Germany

The drought intensities and drought magnitudes are dimensionless measures to estimate the severity of a drought over a specific period or for a specific region. The length of the drought period and the absolute dryness over time are included in the calculation. In comparison to the drought magnitudes, the drought intensity is also normalized over time (i.e. the days of the vegetation period). This means that the drought intensity can reach a maximum value of 0.2 (*Dürren 1952 - 2022 (Jährlich) - Helmholtz-Zentrum Für Umweltforschung UFZ, n.d.*).

The following Figure 8 and Figure 9 show drought intensities and drought magnitudes in the growing season (April to October) for each 4x4km grid cell for the years 1981 - 2022. For the entire soil, the actual soil thickness is shown in the drought monitor, however, it is only up to a maximum depth of 2 meters.

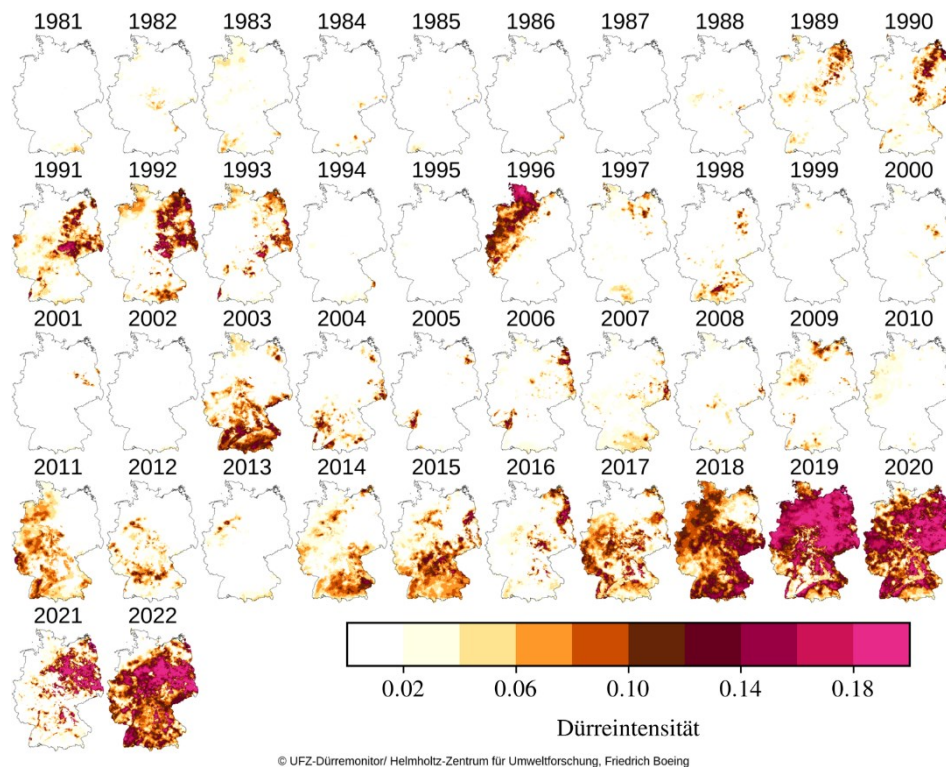
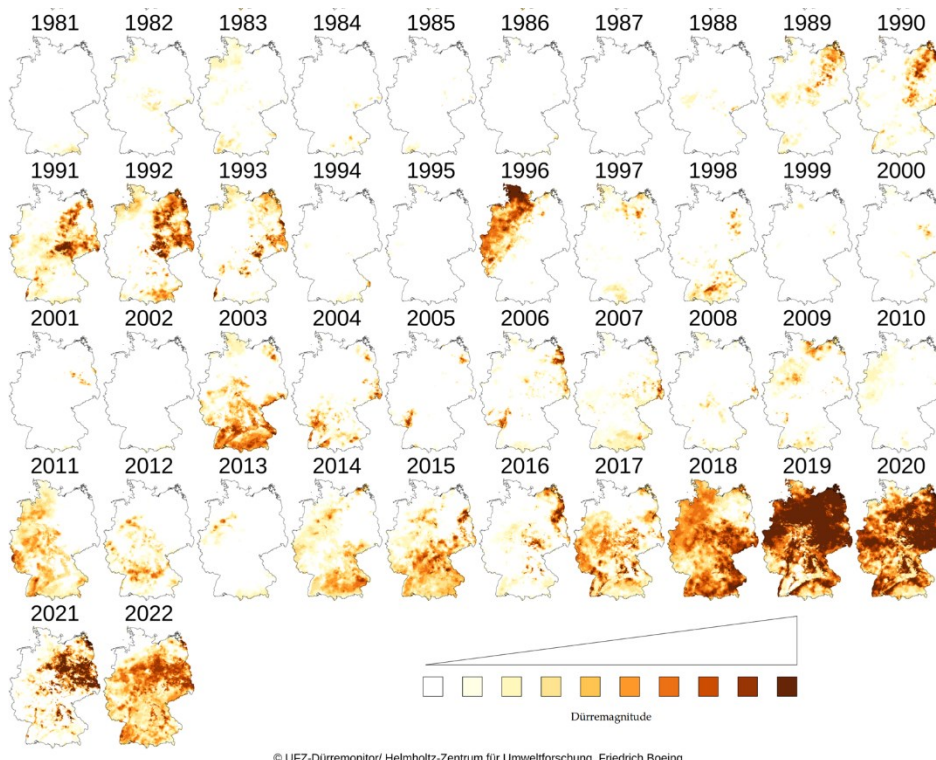


Figure 8. Drought intensities in the growing season from April to October (1981-2022) (*Dürren 1952 - 2022 (Jährlich) - Helmholtz-Zentrum Für Umweltforschung UFZ, n.d.*)



© UFZ-Dürremonitor/ Helmholtz-Zentrum für Umweltforschung, Friedrich Boeing

Figure 9. Drought magnitudes in the April to October growing season (1981-2022) (Dürren 1952 - 2022 (Jährlich) - Helmholtz-Zentrum Für Umweltforschung UFZ, n.d.)

5. Result analyses

5.1. Indices statistics

The study is based on indices that are commonly used for vegetation condition monitoring (Buczyńska & Blachowski, 2021; Karan et al., 2016; Kuzevic et al., 2022). These are NDVI, EVI2 and SAVI.

After calculating the indexes for all the scenes, zones were added to the project as new layers. The zones were selected based on: way of reclamation, year of reclamation and availability of vegetation data. The year of extraction and reclamation, as well as the way of reclamation and the type of vegetation were determined based on the documents provided by MiBRAG, Period of mining was presented on Figure 10.

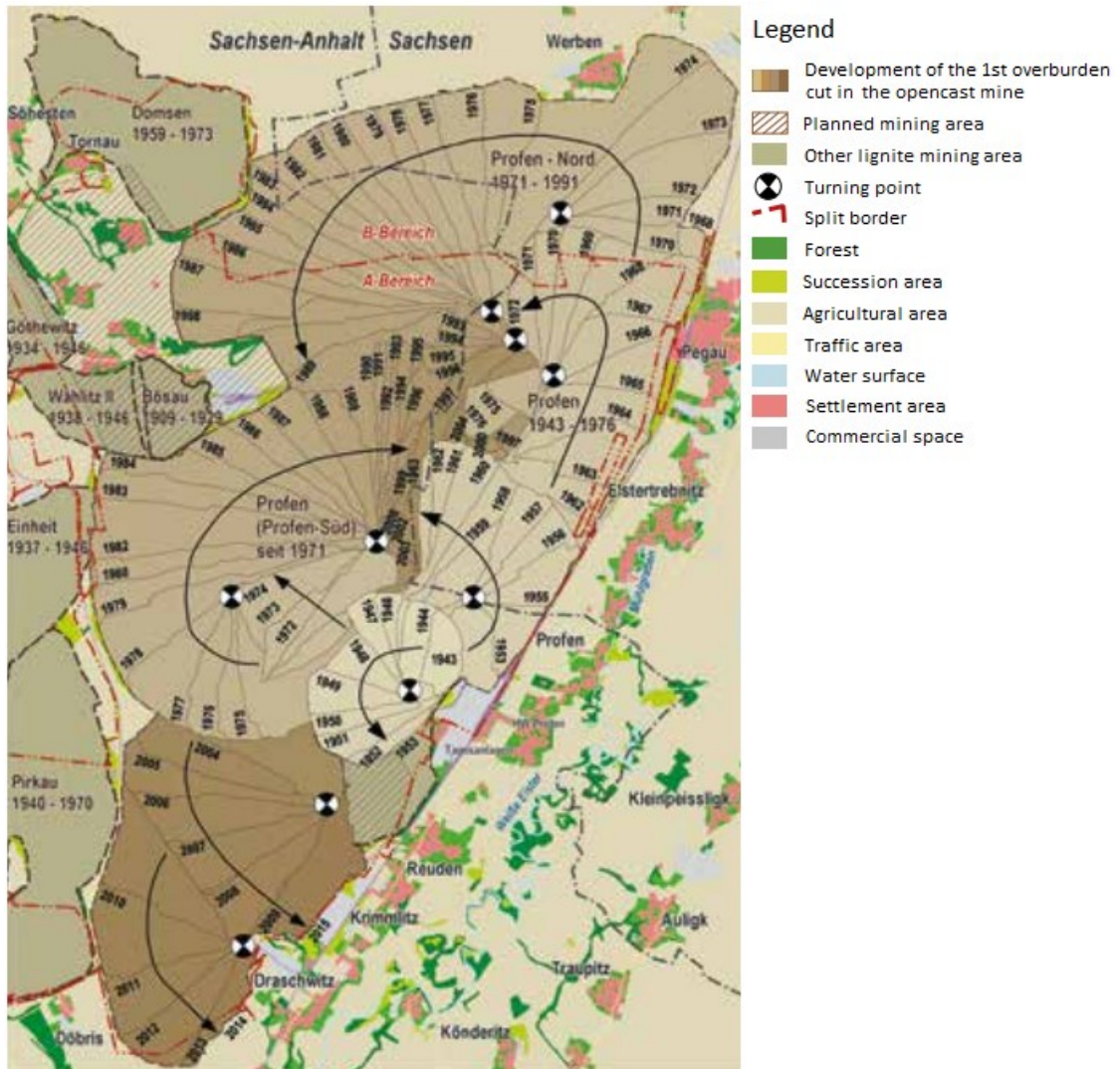


Figure 10. Mining area of Profen with zoning plan (Braunkohlenrevier, n.d.)

Selected zones represent several stages of reclamation within the post-mining landscape. Zone 1 was reclaimed in 2003 and zone 2 in 1994, in both zones mining took place in the years 1940-1970. Zone 3 was reclaimed in 2018. Zone 4 was reclaimed in 1976 and according to Figure 10 is a planned mining area. Apart from reclaimed post-mining sites two reference areas were chosen. Zone 5 covered with forest located beyond the extent of the mine and zone 6 located within the mine. Until the late 1980s, zone 6 was used as agricultural land, and mining began in 1987. Non reclaimed, area underwent natural reclamation and landscaping processes. Single points were selected within the limits of the selected study zones. The specific locations within these zones they were chosen randomly. Figure 11 presents those study zones.

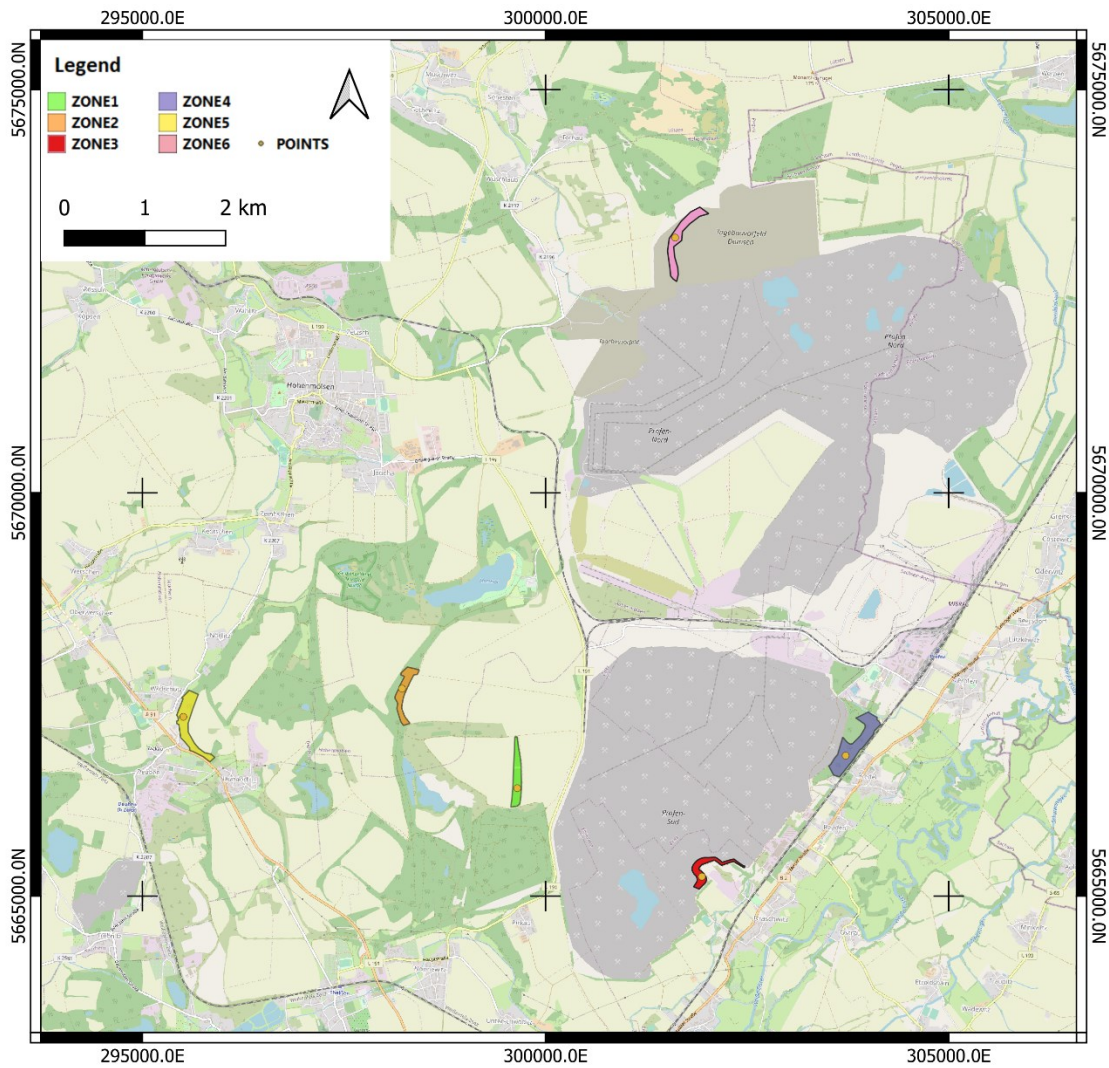


Figure 11. Location of the post-mining region, study zones and points

The vegetation data provided by MIBRAG Company were collected and summarized for each zone (apart from reference ZONE5) in Table 6. Data describe the area size, type of vegetation, trees species and age of vegetation.

Table 6. Summary of vegetation information for study zones

	Area	Forest type	Forest inventory	Condition and age
ZONE1	6,98 ha	Oak type with a high proportion of deciduous trees >20%	<i>Quercus petraea</i> , <i>Tilia cordata</i> , <i>Carpinus betulus</i> , <i>Sorbus aucuparia</i> , <i>Cornus sanguinea</i> and fruit trees	Young growth, in rows or strips, 15-10 years old
ZONE2	7,05ha	Oak type with a high proportion of deciduous trees >20%	<i>Quercus petraea</i> , <i>Tilia cordata</i> , <i>Acer pseudoplatanus</i> , Hybrid form of <i>Populus species</i> , <i>Betula pendula</i> , <i>Carpinus betulus</i> , <i>Sorbus aucuparia</i> , <i>Cornus sanguinea</i>	Young growth to weak polewood, in rows or strips, 20 years old

	Area	Forest type	Forest inventory	Condition and age
ZONE3	1,64ha		Mostly bareness; planned trees species: <i>Quercus petraea</i> , <i>Carpinus betulus</i> , <i>Tilia cordata</i>	
	1,9ha	Oak type with a high proportion of deciduous trees >20%	<i>Quercus petraea</i> , <i>Tilia cordata</i> , <i>Salix caprea</i> , <i>Acer platanoides</i> , <i>Carpinus betulus</i>	5 years
	2,7ha		Mostly bareness; trees left on the surface: <i>Quercus petraea</i> , <i>Acer platanoides</i> , <i>Carpinus betulus</i> , Planned planting: <i>Quercus petraea</i> , <i>Carpinus betulus</i> , <i>Tilia cordata</i>	
ZONE4		high proportion of deciduous trees >20%	Weak tree wood: <i>Betula pendula</i> , <i>Populus species</i> , <i>Robinia pseudoacacia</i> , <i>Acer platanoides</i> ; Other shrub species	60years +/- 10years; 10 years
ZONE6		high proportion of deciduous trees >20%	Weak polewood: <i>Betula pendula</i> , <i>Pinus sylvestris</i> , Hybrid form of <i>Populus species</i> , <i>Robinia pseudoacacia</i>	Around 15 years +/- 5years

Chart presented on Figure 12 combined with the information obtained from MIBRAG Company presented in Table 6 gives an insight on differences in spectral reflectance for various species. Some of the species discussed in the publication by Maschler et al., 2018, overlap with the species in this study (*Quercus petraea* and *Betula pendula*).

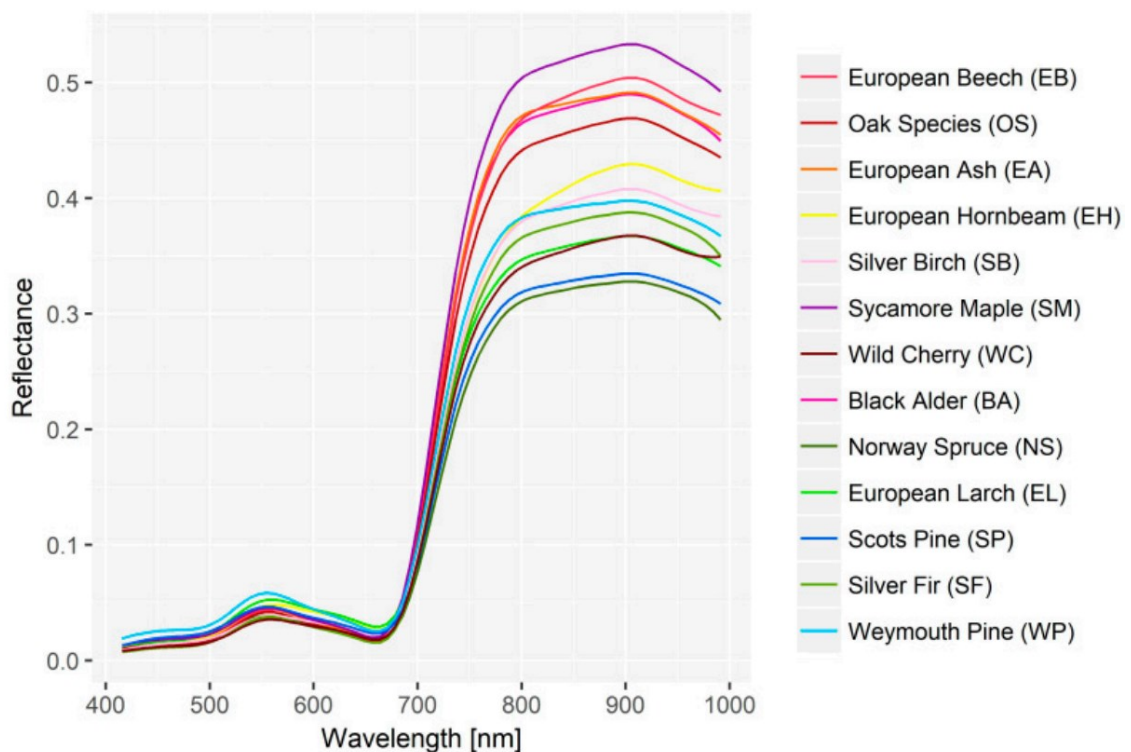


Figure 12. Average spectral signatures of the 13 tree species (Maschler et al., 2018)

The reflectance values of the different species are particularly widespread around wavelengths > 800 nm. The reflectance of Oak Species (*Quercus*) is comparatively high, while the average value among all species is shown by birch (*Betula*). Finding the differences in reflectance values for various tree species might later explain the changes in values of spectral indexes.

5.1.1. Monthly statistics

Rasters with mean values for month July for each year were created using GRASS r.series. The purpose of analyzing rasters of average monthly values is to detect and identify general temporal changes within the zones of the study area.

Comparison of the results throughout the years enables identification of areas that changed over time. Additional image comparison provides insight into reclamation progress. From looking at the generated maps it is possible to easily detect mine site, as it presents itself as barren land with low index values. In case of NDVI, the values oscillate in the range from 0 to 0,15. For EVI2 and SAVI the obtained results are similar and for barren land reach 0,25. The mining area is characterised by low NDVI values, due to the lack of vegetation. Objects such as puddles and small pools of water are reflected in negative vegetation index values, reaching values near to -1. For NDVI healthy vegetation in this case presents with value range 0,35-0,6. The results for SAVI and EVI2 vary a little and the range for healthy vegetation is 0,55-0,85. Detailed comparison is presented in appendices 1A-1E, 2A-2E and 3A-3E.

Statistics including mean value and standard deviation were derived using the Zonal Statistics tool for each zone. Data was extracted and processed in excel. The results were presented on charts.

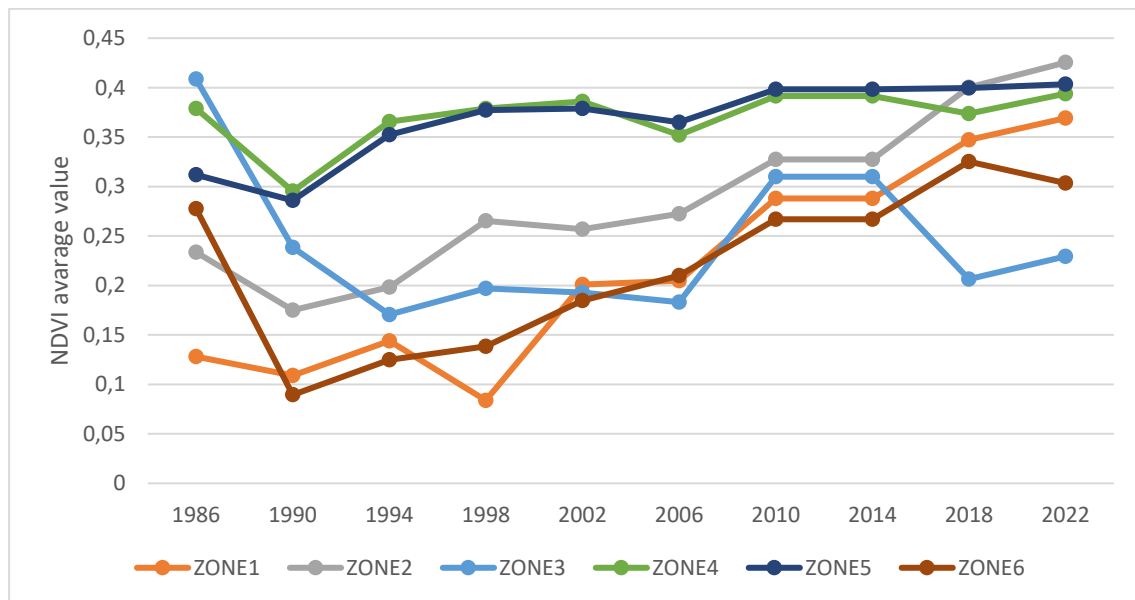


Figure 13. Mean NDVI values in years 1986-2022

The values of NDVI vary depending on the zone (Figure 13). The most stable is ZONE4, reclaimed in the 1970s', the values vary slightly between 0,295 and 0,394. Apart from ZONE4, the reference ZONE5, which has vegetation undisturbed by mining, looks very stable, with values ranging from 0,286 to 0,403. Similar average NDVI values and a trend in time of ZONE4 in relation to the reference ZONE5 testify to the good condition of the reclaimed zone in the 1970s. The highest average value, which is 0,425, presented on the

chart belongs to ZONE2, reclaimed in 1994. Decrease from 1986 to 1990 was caused by getting rid of self-sown seedlings from non-reclaimed, post-mining areas. ZONE3 has been the mine boundary since 2014. In 2018, reclamation was carried out and the chart shows a slight improvement from 0,207 to 0,229. Before the start of mining works, it belonged to agricultural land. In the years preceding the mine's affiliation, the changes in the average NDVI values were conditioned by changes in crops. In ZONE1 until the mid-1990s self-sown plants grew there, the noticeable change from year 1994 to year 1998 is due to the removal of self-sown vegetation. In 2002 the reclamation was completed, that's why a slight increase of mean NDVI value from 0,201 to 0,205 in 2006, and later in 2010 to 0,288.

A steady increase in average values can be seen, which indicates an improvement in the state of vegetation in ZONE1, ZONE2 and ZONE6. Unfortunately, the same cannot be said for ZONE3, which due to recent mining activity has not been able to regenerate.

Higher values in case of ZONE2, as well as ZONE1 might be connected with younger vegetation but also with a type of species (*Quercus petraea*) that dominates those zones and is characterized by a higher reflectance (Figure 12).

Low values might be caused by the presence of small pools of water or patches of dry land within the borders of chosen zones.

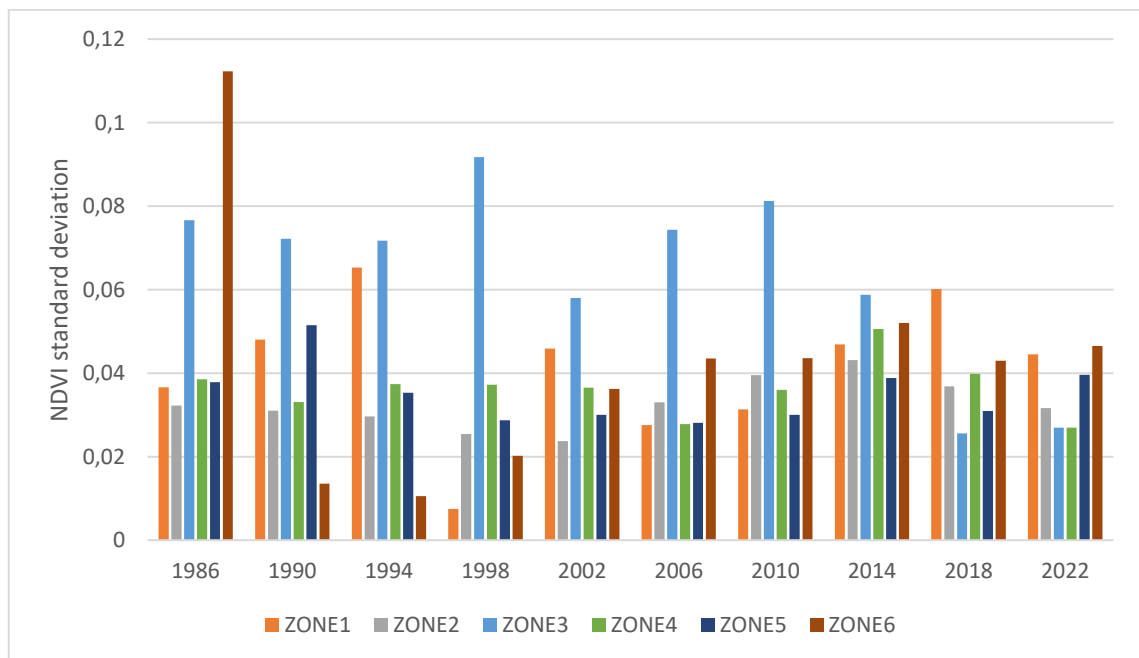


Figure 14. Standard deviation of NDVI in years 1986-2022

The diversity of vegetation and its condition, represented as mean NDVI values, are described by standard deviation. The standard deviation of NDVI is diverse in ZONE1, ZONE3 and ZONE6 (Figure 14). The largest deviation is observed in ZONE6, that's due to getting rid of vegetation, at the cost of starting mining works. The highest value of 0,112 is observed in 1986, at the same time it is an outlier value. The NDVI of vegetation in ZONE5 and ZONE6 is the least dispersed.

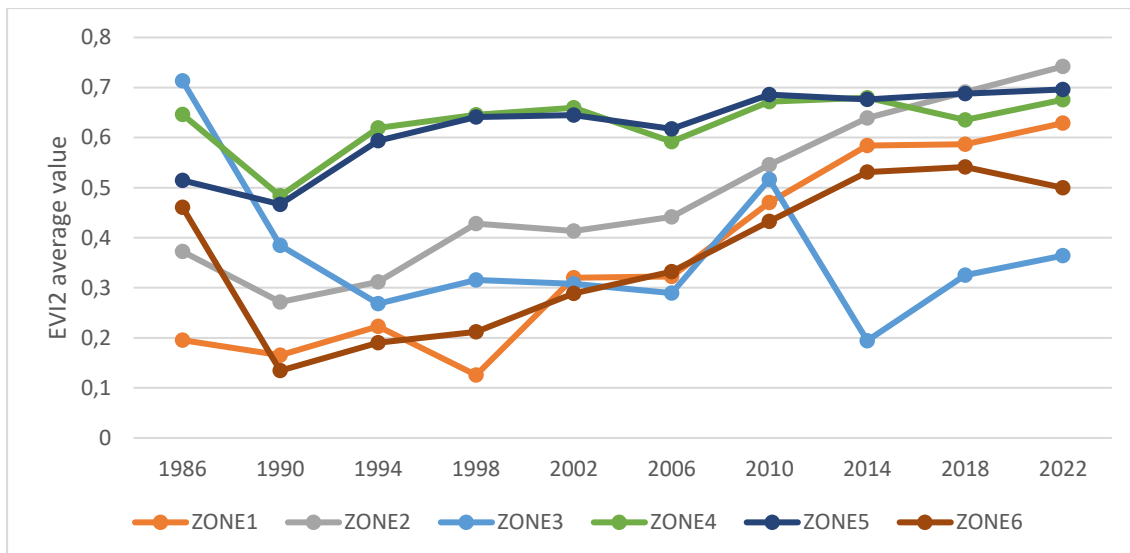


Figure 15. Mean EVI2 values in years 1986-2022

The EVI2 values range from 0,126 in ZONE1 to 0,742 in ZONE2 (Figure 15). In the zone restored in 1994, the EVI2 increases value in 1998, reaching 0,428. In the next time stamp, there is a decrease to the level of 0,413, in the upcoming years it will get better. EVI2 values for ZONE4 and the reference ZONE5 look similar. They both seem stable, apart from that, a slight increase can be noticed, which indicate improvement in vegetation's condition. EVI2 values differ from NDVI values of ZONE3, in EVI2 values, a significant deterioration from 2010 to 2014 is noticeable, it may be due to the start of mining activities. ZONE6, that was left without restoration, from 1994 is showing increase in EVI2 value.

ZONE1, ZONE2 and ZONE6 show an improvement in vegetation status through a steady increase in mean EVI2 values.

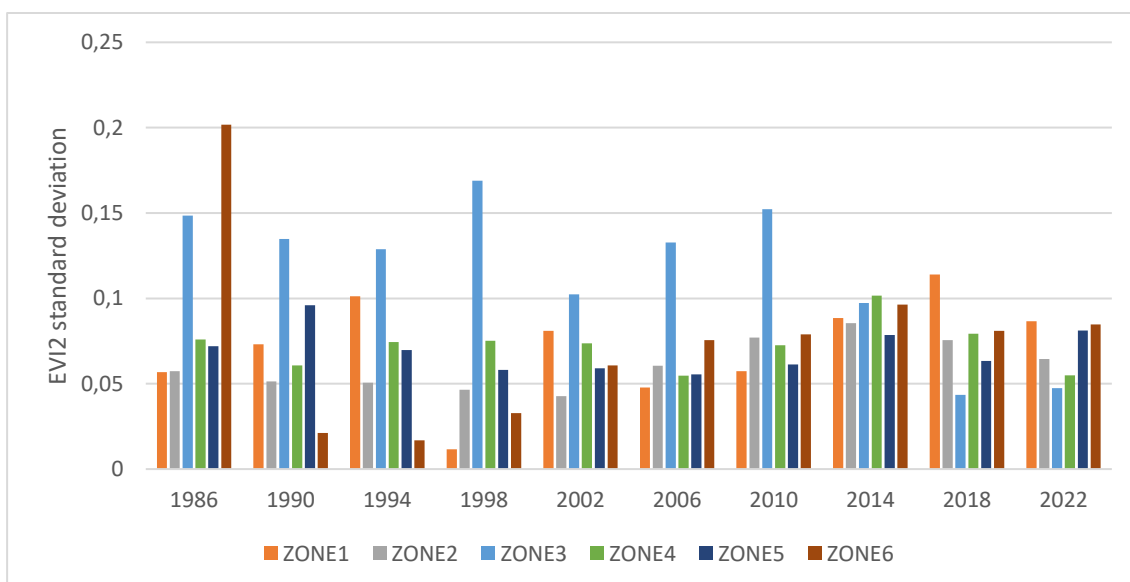


Figure 16. Standard deviation of EVI2 in years 1986-2022

The standard deviation of the EVI2 in ZONE2, ZONE4 and ZONE5 is on a stable level, which indicates low variety within the zone (Figure 16). The largest fluctuations of values occur in the non-reclaimed region, where the standard deviation varies from 0.202 to

0.021. It suggests the time of starting mine works. For ZONE1 there is also an aberration in 1998 when the standard deviation is significantly lower.

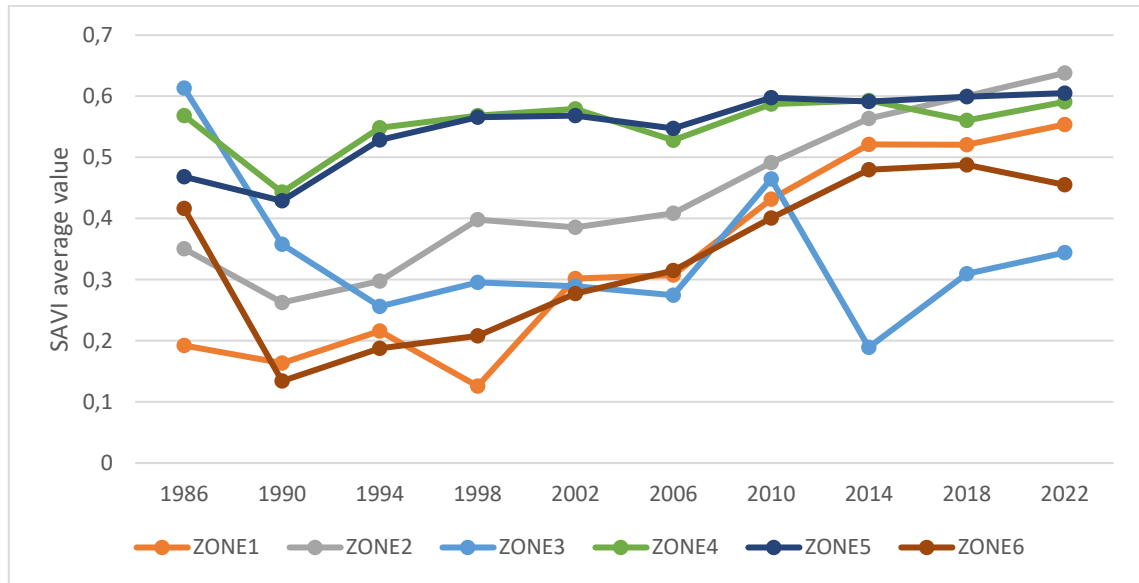


Figure 17. Mean SAVI values in years 1986-2022

The lowest SAVI values presented in the chart belong to ZONE1 (0,126), ZONE3 (0,189) and ZONE6 (0,134) (Figure 17). These values are conditioned by the commencement of mining operations or, in the case of ZONE1, technical recultivation and land preparation for tree plantings. For ZONE2, there is a slight increase, referring to reclamation process finished in 1994. The values of SAVI for ZONE4 and 5 are stable with a slight increase. They share similar SAVI values, which means the condition of trees and other vegetation is comparable. Steady increase in average values can be seen for ZONE1, ZONE2 and ZONE6, which indicates an improvement in the state of vegetation.

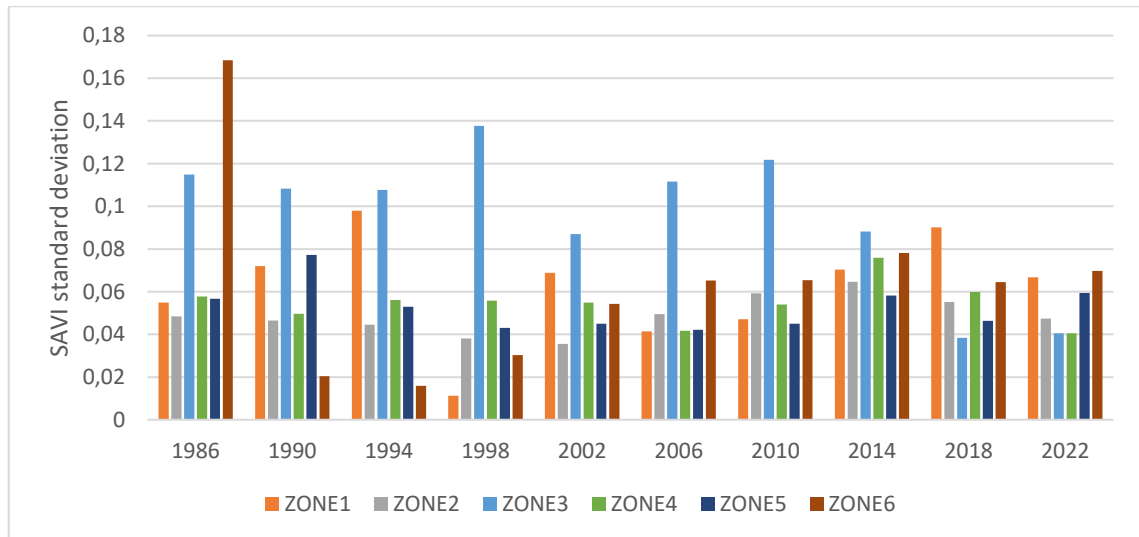


Figure 18. Standard deviation of SAVI in years 1986-2022

The lowest variability of standard deviation is observed in ZONE2, ZONE4 and ZONE5 (Figure 18). It indicates a constant vegetation cover, which consists of different plant species. The largest fluctuations of values occur again in the non-reclaimed region, where the standard deviation varies from 0,168 to 0,020. For ZONE3 noticeable changes are in 2018 where the value from 0,088 decreases to 0,038.

5.1.2. Monthly statistics for single zone points

Single points/pixels were selected in new layers, within the limits of the selected study zones, The specific locations within these zones were chosen randomly. Each pixel value was calculated for every year using Point Sampling Tool. For NDVI the result was presented on the chart (Figure 19).

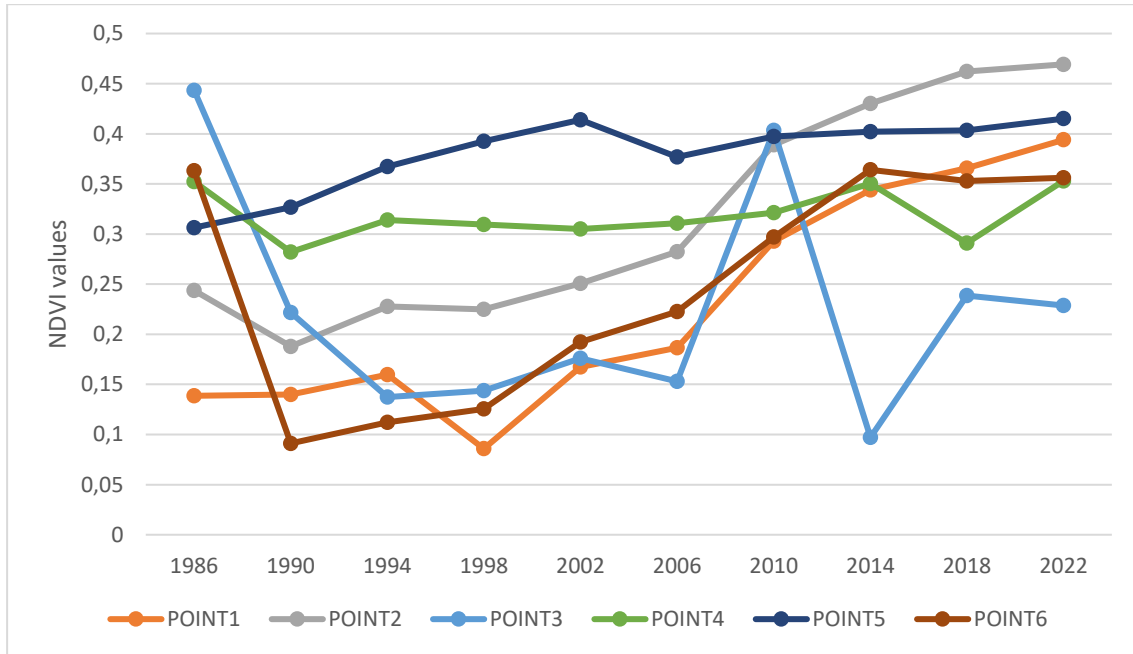


Figure 19. NDVI value for point in years 1986-2022

Comparing the results from single point values with the results from mean zone values, in some cases there is a noticeable difference. The difference may be due to the fact that the previous analysis deals with averaged values and here the values for a single pixel are presented. This means that if there are areas with water or bare soil in a given zone, they affect the average value. The highest NDVI value of 0,469 corresponds to point 2 in 2022. For majority of points the highest values of NDVI fall in 2022. The value 0,086 is the lowest one on the chart, it belongs to point 1, the cause of low value may be preparation for technical recultivation and land preparation for tree plantings. The NDVI values for ZONE4 and ZONE5 are stable.

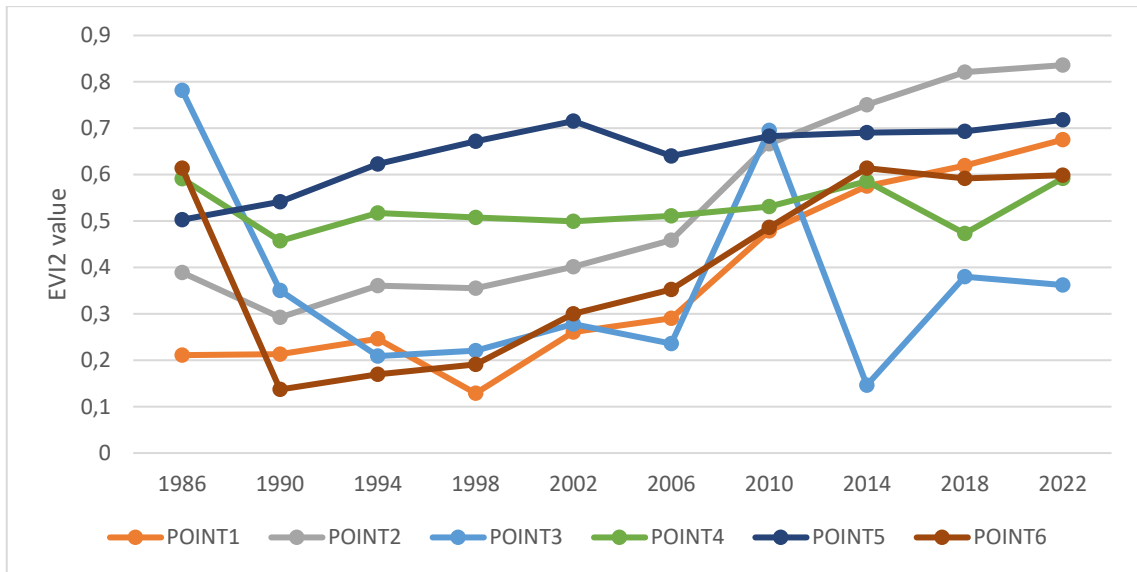


Figure 20. EVI2 value for point in years 1986-2022

Point EVI2 values (Figure 20) in comparison to zonal EVI2 values don't differ strongly. It's because EVI2 is used to correct the effects of soil signals, especially in areas with dense crowns. The highest EVI2 value corresponds to point 2 in 2022. For half of points the highest values of EVI2 fall on 2022. The value 0,129 is the lowest one on the chart, it belongs to point 1.

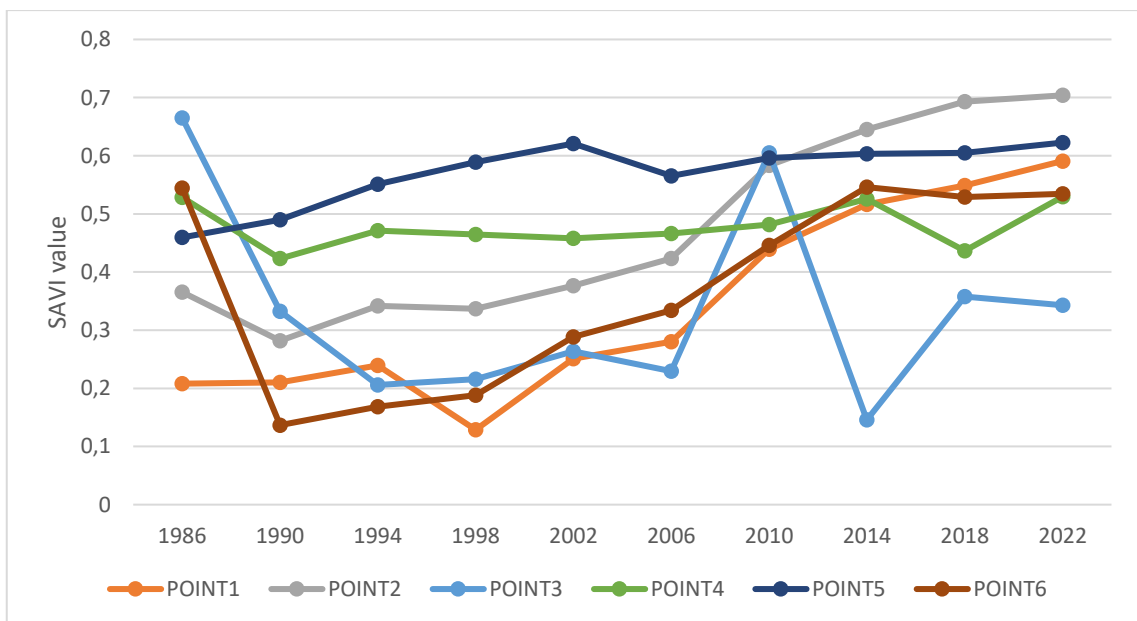


Figure 21. SAVI value for point in years 1986-2022

Point SAVI values (Figure 21) in comparison to zonal SAVI values don't differ strongly. It's due to ability of SAVI to identify soil-induced changes in vegetation indices. It minimalizes soil-brightness influences.

The highest SAVI value (0,704) corresponds to point 2 in 2022, which might prove that the state of vegetation has improved, regardless of the droughts in recent years.

5.1.3. Differential rasters

Based on the monthly average values, the difference between the state in July 2022 and July 1986 is calculated using *Raster Calculator*. Differential rasters for month July were created using raster calculator. The purpose of this calculation is to obtain information about temporal and spatial changes in the conditions of the post-mining landscape. Differential rasters are presented in Figure 22, Figure 23 and Figure 24 for NDVI, EVI2 and SAVI respectively.

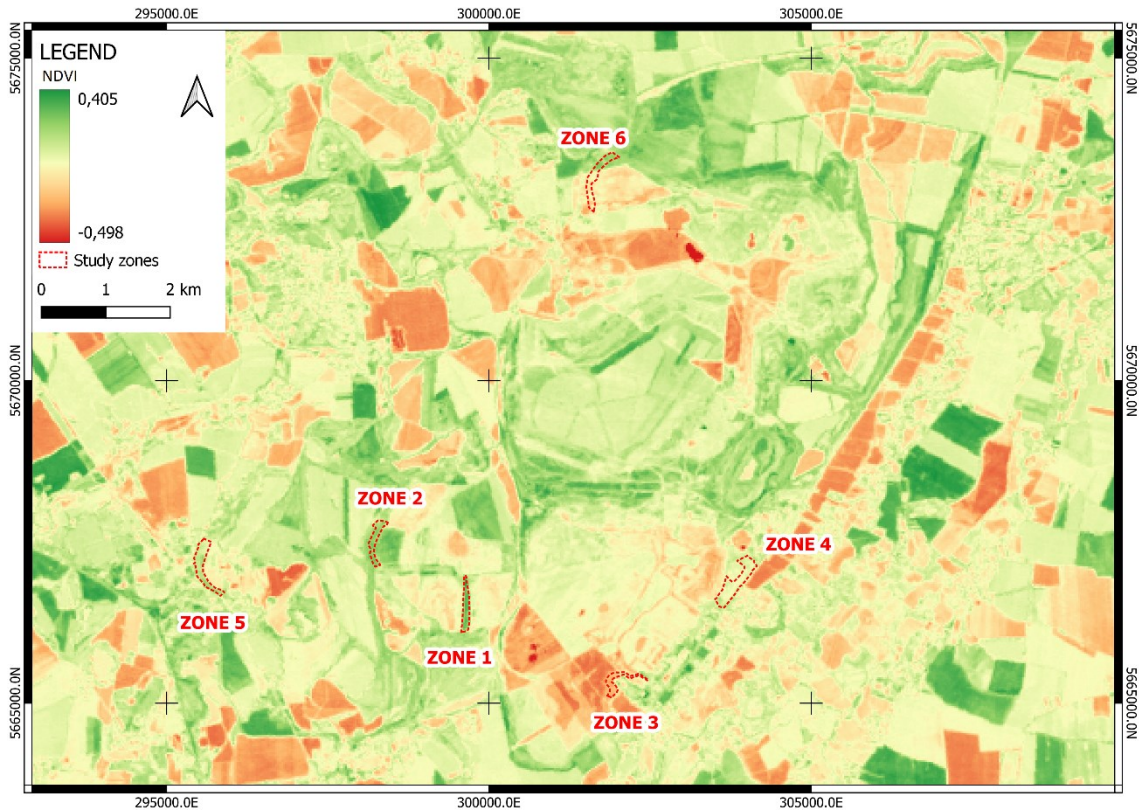


Figure 22. Difference raster of the NDVI values in 1986-2022

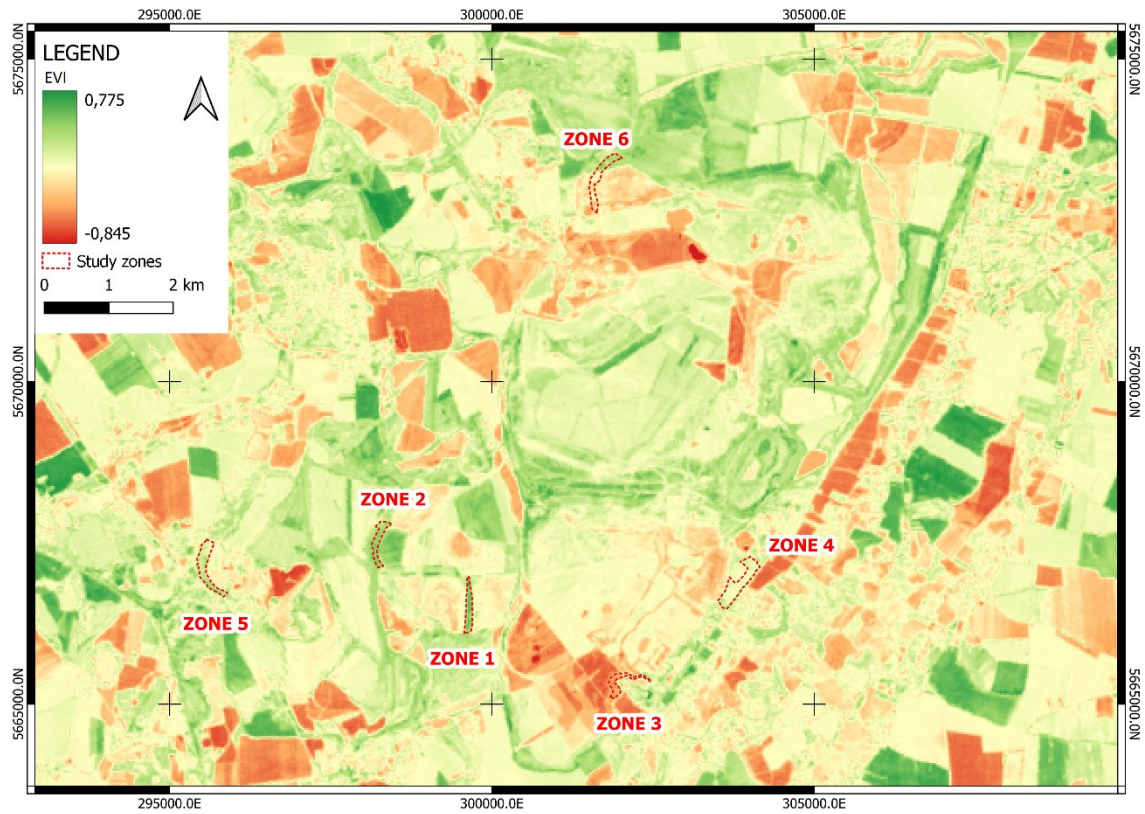


Figure 23. Difference raster of the EVI2 values in 1986-2022

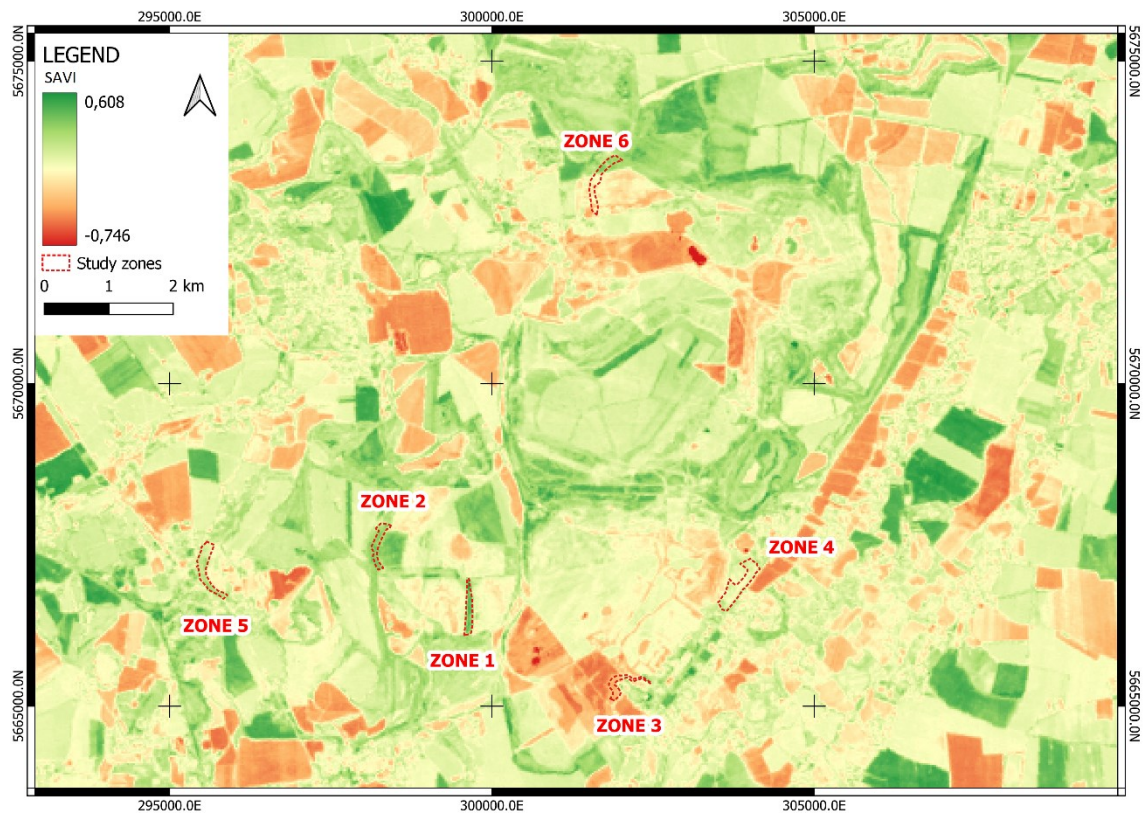


Figure 24. Difference raster of the SAVI values in 1986-2022

The difference rasters of the indexes values for the period of 1986-2022 show similar change trajectories and spatial dependencies.

The majority of area presented in Figure 22, Figure 23 and Figure 24 the difference between 2022 and 1986 generally fluctuates around 0.

5.1.4. Discussion

Temporal profiles of the indices across the study areas exhibit comparable trends and patterns. It is therefore possible to compare and analyze the results together to gain a comprehensive understanding of the region. The range of valid values for NDVI and SAVI, analysed in sections 5.1.1 and 5.1.2 is from -1 to 1.

One of the problems is the range of EVI2, which ranges from -0,4 to 1,2 (Figure 15). Bright features such as clouds and white buildings, along with dark features such as water, can result in anomalous pixel values in an EVI2 image. In spite of this, the EVI2 results are comparable to those of other indexes. NDVI is widely used together with other indices. In moderately vegetated arid areas, such as post-mining landscapes one of the recommended indexes is SAVI. It is adjusted to mitigate the influence of bare soil. EVI2 takes atmospheric factors into account.

The calculation of average annual values was not possible due the low availability of data and the four-year interval was chosen to better represent changes in the landscape. However, depending on the area of interest, the time range might be different or reduced when going into a more detailed analysis. In this case, choosing one month (July), allowed to formulate the basic properties of vegetation in region, adjacent to the mine and to determine time dependencies. Fortunately, selected month is usually characterized in high chlorophyll content for most plants. The reference area, not related to the mine, as well as the area reclaimed in the late 1970s', are covered with healthy vegetation, as evidenced by constant and higher values of vegetation indices. According to the analyses, all zones, apart from zone 3, show an improvement in the condition of the vegetation over the years. Zone 3, which in recent years has been transformed from agricultural land into mining land, was reclaimed in 2018. Currently, the saplings on it are no older than 5 years. The droughts prevailing in the years 2018-2022 could have caused the deterioration of the newly reclaimed land, which is why the growth of new vegetation, as can be seen on the index charts, was not so active. The NDVI chart (Figure 13) showed a deterioration in the condition of vegetation in the reference zone 6 in 2022. Comparing the years 2014, 2018 and 2022, it can be seen that not only the reference zone suffered damage due to the prevailing droughts.

The difference rasters presented in 5.1.3 show similar change trajectories and spatial dependencies. Additional evaluation of coefficient of variation achievable through QGIS software with the use of *r.series* tool could characterize spatial variability.

Unfortunately, no in-situ data was available for the above analysis. However, the study had the opportunity to use the information about the plant species presented in 5.1. The spectral characteristics of plants (trees) were learned from the literature and used for data analysis.

6. Conclusions

The study was aimed at collecting information related to the monitoring of reclaimed land belonging to the mine in order to create an appropriate course of action to support such monitoring.

The first part of the thesis included literature study, one of which purpose was to briefly describe impacts of mining on the environment and post-mining landscapes. Further, the

reclamation aspects were discussed, such as steps and ways of reclamation. In the following chapters, it was possible to see that the need to monitor mining and post-mining areas is justified by many laws and European Union reports and directives.

Related aim of this study was to investigate the relevant spectral indices with the intention to use them for designing a project workflow that is useful for monitoring the health and condition of reclaimed post-mining landscapes. The following indexes were selected: NDVI, EVI2 and SAVI. The research focused on satellite data and multispectral imagery resulted in selecting several Landsat satellite missions. They were selected based on the ability to offer data dating back to the 1970s. The study was carried out on a chosen opencast mine located in Profen, Germany. The investigated period covered vegetation season in years 1986-2022, in the form of a four-year interval.

Monitoring was conducted in QGIS, which is free and open-source software. The satellite images were preprocessed. Multiraster layers were created with QGIS software. Six study zones were selected within the mine area, based on forest way of reclamation. Rasters of average monthly and annual values were generated and compared using time series analysis. Other products of this part were differential rasters, the created maps of changes subjected to statistical analysis, determining the general area, where there was a decrease or increase in the vegetation index, were used for a detailed visual analysis.

The conducted time series analysis confirmed the stability in one of the reference zones, not belonging to the mine. Average values of the indexes were mostly stable, with higher levels, suggesting healthy vegetation. In the post-mining region, indexes values were distributed in a more diverse manner over time. In the second reference zone, non-reclaimed post-mining land, was behaving better than expected, the vegetation found its way and has improved throughout the years. Zone 3 well reflects the changes taking place in its area, the change of use. Zones 1 and 2 noted a constant increase in vegetation health throughout the analysis period. It took respectively 20 and 15-10 years for the new vegetation planted in 1994, 2003 to reach similar NDVI values as the vegetation in the undisturbed environment.

In addition, the study took into account archival information on droughts occurring in Germany, which could have had a negative impact on vegetation. Universal value decrease can be found in 1990 and 2006. Decrease in 1990 can be related to drought occurring in the study area. Unfortunately, this cannot be said for 2006, as the fall could have been caused by an error in the satellite image, this year only one scene was found corresponding to the study.

This study faced a number of limitations and issues during the practical portion. One of the problems was the unavailability of most of the scenes. Due to the high cloud coverage, many of satellite images was rejected. As a result, the study focused only on July, as it was the month with the largest amount of data, with data throughout the whole analysis period, apart from one day. Second problem was the age and type of data. Due to the use of Landsat 4-5 data, some spectral bands are missing, which prevents some indexes from being used.

Mineral extraction is associated with disturbance of vegetation in the surrounding area that might lead to loss of valuable habitats. The study showed potential of using remote sensing data for evaluating condition of reclaimed forests. The suggested workflow was based on comparing post-mining reclaimed zones using three spectral indices (NDVI, EVI2 and SAVI). The index analyses characterized condition of vegetation throughout years (1986-2022). In addition, the analyzes were compared with archived data on

droughts and data on tree species. The collected data made it possible to understand how various factors affect the state of plant vegetation. The proposed methodology with the use of spectral satellite data is a preliminary approach to the subject, which allows for digressions and the development of the scope of analyzes and collected data in the future. Using selected indicators, it's possible to design the monitoring of areas that will be subject to reclamation and propose that in-situ data be collected at the same time and to a lesser extent, because satellite images for the entire reclaimed area can be used based on in-situ correlation with remote sensing.

7. Future recommendations

In order to improve the results of the analysis of the state of the environment in a given area in the future and to gain a wider perspective on the health of the vegetation, more indexes analysis should be considered, e.g., water indexes like NDWI or NDMI, so as to identify the factors that influenced a given change in the state of vegetation (e.g., lack or excess of water, late start of the season growing season, natural changes during the growing season). Additionally, to improve analysis more years and wider spectrum of vegetation months should be investigated and compared. Future research should also consider adding images from other sensors. This would allow for a wider time coverage, which is very important when detecting and forecasting long-term trends.

In order to assess ecosystem development on a large scale, long-term ground monitoring data should be integrated with remote sensing metrics, since comprehensive ground monitoring data sets are often required by regulators to demonstrate rehabilitation progress. Remote sensing images provided by satellites should be supported by the unmanned aerial vehicle (UAV) sensors and platforms that nowadays are being used in almost every application (e.g., agriculture, forestry, and mining). The UAV are equipped with hyperspectral cameras that are becoming more available.

Although remote sensing monitoring has been used for more than 50 years, there is still no scientific consensus on how to determine the success of rehabilitation with the use of remote sensing.

8. Bibliography

- Acharya, T. D., Subedi, A., & Lee, D. H. (2018). Evaluation of water indices for surface water extraction in a landsat 8 scene of Nepal. *Sensors (Switzerland)*, 18(8). <https://doi.org/10.3390/s18082580>
- Advanced Spaceborne Thermal Emission and Reflection Radiometer - Wikipedia*. (n.d.). Retrieved January 24, 2023, from https://en.wikipedia.org/wiki/Advanced_Spaceborne_Thermal_Emission_and_Reflection_Radiometer
- Asr, E. T., Kakaie, R., Ataei, M., & Tavakoli Mohammadi, M. R. (2019). A review of studies on sustainable development in mining life cycle. *Journal of Cleaner Production*, 229, 213–231. <https://doi.org/10.1016/J.JCLEPRO.2019.05.029>
- Bannari, A., Morin, D., Bonn, F., & Huete, A. R. (1995). A review of vegetation indices. *Remote Sensing Reviews*, 13(1–2), 95–120. <https://doi.org/10.1080/02757259509532298>

- Biomass - Earth Online*. (n.d.). Retrieved February 2, 2023, from <https://earth.esa.int/eogateway/missions/biomass>
- Braunkohlengesellschaft mbH MIBRAG, M., & Kappa GmbH, A. (n.d.). *MIBRAG – Tagebau Profen Besucherinformation*.
- Braunkohlenrevier, M. (n.d.). *A Profen Profen Wandlungen und Perspektiven*.
- Buczyńska, A. (2020). Badania komponentów środowiska przyrodniczego na obszarach pogórnicych z wykorzystaniem wysokorozdzielczych zobrażeń satelitarnych. *Przegląd Górniczy*, 76(3), 1–7.
- Buczyńska, A., & Blachowski, J. (2021). Analysis of the vegetation condition on the area of the closed Babina mine in 1989-2019 using multispectral satellite images. *IOP Conference Series: Earth and Environmental Science*, 684(1). <https://doi.org/10.1088/1755-1315/684/1/012030>
- Cerin, P. (2006). Bringing economic opportunity into line with environmental influence: A discussion on the Coase theorem and the Porter and van der Linde hypothesis. *Ecological Economics*, 56(2), 209–225. <https://doi.org/10.1016/j.ecolecon.2005.01.016>
- Chen, J. M. (1996). Canopy architecture and remote sensing of the fraction of photosynthetically active radiation absorbed by boreal conifer forests. *IEEE Trans. Geosci. Remote. Sens.*, 34, 1353–1368.
- Classification Algorithms and Methods*. (n.d.). Retrieved March 6, 2023, from https://seos-project.eu/classification/classification-c01-p05.html?fbclid=IwAR0ztAWDCvGa9GtxAPaphBjEUiRQrPSIQvOI_MoatidniPwLP7nznduKm20
- de Jong, R., de Bruin, S., de Wit, A., Schaepman, M. E., & Dent, D. L. (2011). Analysis of monotonic greening and browning trends from global NDVI time-series. *Remote Sensing of Environment*, 115(2), 692–702. <https://doi.org/10.1016/J.RSE.2010.10.011>
- Dernbach, J. C. (1998). Sustainable Development as a Framework for National Sustainable Development as a Framework for National Governance Governance CASE WESTERN RESERVE LAW REVIEW ARTICLES SUSTAINABLE DEVELOPMENT AS A FRAMEWORK FOR NATIONAL GOVERNANCE. *Case Western Reserve Law Review*, 49. <https://scholarlycommons.law.case.edu/caselrevhttps://scholarlycommons.law.case.edu/caselrev/vol49/iss1/3>
- Dernbach, J. C. (2003). Indiana Journal of Global Legal Studies Studies Achieving Sustainable Development: The Centrality and Multiple Achieving Sustainable Development: The Centrality and Multiple Facets of Integrated Decisionmaking Facets of Int. In *Indiana Journal of Global Legal Studies* (Vol. 10, Issue 1). <https://www.repository.law.indiana.edu/ijgls/vol10/iss1/10>
- DLR - Earth Observation Center - DESIS*. (n.d.). Retrieved January 16, 2023, from <https://www.dlr.de/eoc/en/desktopdefault.aspx/tabid-13614/>
- Dürren 1952 - 2022 (jährlich) - Helmholtz-Zentrum für Umweltforschung UFZ*. (n.d.). Retrieved March 2, 2023, from <https://www.ufz.de/index.php?de=47252>

- Dvorakova, K., Heiden, U., & van Wesemael, B. (2021). Sentinel-2 exposed soil composite for soil organic carbon prediction. *Remote Sensing*, 13(9). <https://doi.org/10.3390/rs13091791>
- Dwivedi, R. S. (2017). Remote sensing of soils. *Remote Sensing of Soils*, 1–462. <https://doi.org/10.1007/978-3-662-53740-4/COVER>
- EarthExplorer*. (n.d.). Retrieved February 22, 2023, from <https://earthexplorer.usgs.gov/>
- Eitel, J. U. H., Keefe, R. F., Long, D. S., Davis, A. S., & Vierling, L. A. (2010). Active Ground Optical Remote Sensing for Improved Monitoring of Seedling Stress in Nurseries. *Sensors 2010, Vol. 10, Pages 2843-2850*, 10(4), 2843–2850. <https://doi.org/10.3390/S100402843>
- ELAW - Environmental Law Alliance Worldwide. (2010). Overview of Mining and Its Impacts. *Guidebook for Evaluating Mining Project, Eugene*. <https://www.elaw.org/files/mining-eia-guidebook/Full-Guidebook.pdf>
- Erener, A. (2011). Remote sensing of vegetation health for reclaimed areas of Seyitömer open cast coal mine. *International Journal of Coal Geology*, 86(1), 20–26. <https://doi.org/10.1016/j.coal.2010.12.009>
- ESA - *The Sentinel missions*. (n.d.). Retrieved January 16, 2023, from https://www.esa.int/Applications/Observing_the_Earth/Copernicus/The_Sentinel_missions
- Five Landsat Quirks You Should Know | Pixalytics Ltd.* (n.d.). Retrieved February 22, 2023, from <https://www.pixalytics.com/landsat-quirks/>
- FLEX - Earth Online*. (n.d.). Retrieved February 2, 2023, from <https://earth.esa.int/eogateway/missions/flex>
- Gadal, S., Gbetkom, P., & Mfondoum, A. (2021). A New Soil Degradation Method Analysis by Sentinel 2 Images Combining Spectral Indices and Statistics Analysis: Application to the Cameroonians Shores of Lake Chad and Its Hinterland. *Proceedings of the 7th International Conference on Geographical Information Systems Theory, Applications and Management*, 25–36. <https://doi.org/10.5220/0010521200250036>
- Gao, B. (1996). NDWI—A normalized difference water index for remote sensing of vegetation liquid water from space. *Remote Sensing of Environment*, 58(3), 257–266. [https://doi.org/https://doi.org/10.1016/S0034-4257\(96\)00067-3](https://doi.org/https://doi.org/10.1016/S0034-4257(96)00067-3)
- GeoEye-1 - Earth Online*. (n.d.). Retrieved January 30, 2023, from <https://earth.esa.int/eogateway/missions/geoeye-1>
- Gitelson, A. A., Kaufman, Y. J., Merzlyak, M. N., & Blaustein, J. (1995). Use of a Green Channel in Remote Sensing of Global Vegetation from EOS-MODIS. In *REMOTE SENS. ENVIRON* (Vol. 58). ©Elsevier Science Inc.
- Gitelson, A. A., Kaufman, Y. J., Stark, R., & Rundquist, D. (2002). Novel algorithms for remote estimation of vegetation fraction. *Remote Sensing of Environment*, 80, 76–87. www.elsevier.com/locate/rse
- Huete, A., Didan, K., Miura, T., Rodriguez, E. P., Gao, X., & Ferreira, L. G. (2002). Overview of the radiometric and biophysical performance of the MODIS vegetation indices. *Remote Sensing of Environment*, 83(1), 195–213. [https://doi.org/https://doi.org/10.1016/S0034-4257\(02\)00096-2](https://doi.org/https://doi.org/10.1016/S0034-4257(02)00096-2)

- Huete, A. R. (1988). A Soil-Adjusted Vegetation Index (SAVI). In *REMOTE SENSING OF ENVIRONMENT* (Vol. 25).
- IDB - Show Indices for selected Sensor. (n.d.). Retrieved January 24, 2023, from https://www.indexdatabase.de/db/is.php?sensor_id=96
- IRS-1C - Earth Online. (n.d.). Retrieved February 2, 2023, from <https://earth.esa.int/eogateway/missions/irs-1c>
- IRS-1D - Earth Online. (n.d.). Retrieved February 2, 2023, from <https://earth.esa.int/eogateway/missions/irs-1d>
- IRS-R2 (ResourceSat-2) - Earth Online. (n.d.). Retrieved February 2, 2023, from <https://earth.esa.int/eogateway/missions/resourcesat-2>
- Jackson, R. D., Slater, P. N., & Pinter, P. J. (1983). Discrimination of Growth and Water Stress in Wheat by Various Vegetation Indices Through Clear and Turbid Atmospheres. In *REMOTE SENSING OF ENVIRONMENT* (Vol. 13).
- Jain, R. K., Cui, Z. “Cindy,” & Domen, J. K. (2016). Chapter 4 - Environmental Impacts of Mining. In R. K. Jain, Z. “Cindy” Cui, & J. K. Domen (Eds.), *Environmental Impact of Mining and Mineral Processing* (pp. 53–157). Butterworth-Heinemann. <https://doi.org/https://doi.org/10.1016/B978-0-12-804040-9.00004-8>
- Jiang, Z., Huete, A. R., Didan, K., & Miura, T. (2008). Development of a two-band enhanced vegetation index without a blue band. *Remote Sensing of Environment*, 112(10), 3833–3845. <https://doi.org/10.1016/J.RSE.2008.06.006>
- Karan, S. K., Samadder, S. R., & Maiti, S. K. (2016). Assessment of the capability of remote sensing and GIS techniques for monitoring reclamation success in coal mine degraded lands. *Journal of Environmental Management*, 182, 272–283. <https://doi.org/10.1016/j.jenvman.2016.07.070>
- Kasprzyk, P. (2009). Kierunki rekultywacji w górnictwie odkrywkowym - Directions of reclamation in surface mining. *Problemy Ekologii Krajobrazu*, XXIV, 7–15.
- Kickler, K., & Franken, G. (2017). *Sustainability Schemes for Mineral Resources a Comparative Overview* (Bundesanstalt für Geowissenschaften und Rohstoffe, Ed.). https://www.bgr.bund.de/EN/Themen/Min_rohstoffe/Downloads/Sustainability_Schemes_for_Mineral_Resources.pdf?__blob=publicationFile&v=6
- Knipfer, A., & Schierack, M. (2018). *Nachweisführung für Maßnahmen zum Natur- und Artenschutz-ein Statusbericht*.
- Köhler, C. (2019). Towards Sentinel 2 based environmental contamination monitoring. 20. *GEOKINEMATISCHER TAG*. <https://scihub.copernicus.eu/dhus/>.
- Kretschmann, J. (2020). Post-Mining-a Holistic Approach. *Mining, Metallurgy & Exploration*, 37, 1401–1409. <https://doi.org/10.1007/s42461-020-00265-y/Published>
- Krutz, D., Müller, R., Knodt, U., Günther, B., Walter, I., Sebastian, I., Säuberlich, T., Reulke, R., Carmona, E., Eckardt, A., Venus, H., Fischer, C., Zender, B., Arloth, S., Lieder, M., Neidhardt, M., Grote, U., Schrandt, F., Gelmi, S., & Wojtkowiak, A. (2019). The Instrument Design of the DLR Earth Sensing Imaging Spectrometer (DESI). *Sensors (Basel, Switzerland)*, 19(7). <https://doi.org/10.3390/S19071622>

- Krzemiński, P. (2021, June 5). *Land reclamation after mining activity (Rekultywacja gruntów po działalności górniczej)*. <https://egornik.pl/rekultywacja-gruntow-po-dzialalnosci-gorniczej/>
- Kuzevic, S., Bobikova, D., & Kuzevicova, Z. (2022). Land Cover and Vegetation Coverage Changes in the Mining Area—A Case Study from Slovakia. *Sustainability (Switzerland)*, *14*(3). <https://doi.org/10.3390/su14031180>
- Land Reclamation in Canada | Land Reclamation Projects & Action | CAPP*. (n.d.). Retrieved January 16, 2023, from <https://www.capp.ca/explore/land-reclamation/>
- Land recultivation * Arable farming*. (n.d.). Retrieved January 16, 2023, from https://universityagro.ru/en/arable-farming/land-recultivation/#Stages_of_land_recultivation
- Landsat 1 | U.S. Geological Survey*. (n.d.). Retrieved January 16, 2023, from <https://www.usgs.gov/landsat-missions/landsat-1>
- Landsat 9 | Landsat Science*. (n.d.). Retrieved January 16, 2023, from <https://landsat.gsfc.nasa.gov/satellites/landsat-9/>
- Landsat Level-2 and Level-3 Science Products | U.S. Geological Survey*. (n.d.). Retrieved March 5, 2023, from <https://www.usgs.gov/media/images/landsat-level-2-and-level-3-science-products>
- Landsat Missions | U.S. Geological Survey*. (n.d.). Retrieved January 16, 2023, from <https://www.usgs.gov/landsat-missions>
- Landsat Satellite Missions | U.S. Geological Survey*. (n.d.). Retrieved January 30, 2023, from <https://www.usgs.gov/landsat-missions/landsat-satellite-missions>
- Lechner, A. M., Owen, J., Ang, M., & Kemp, D. (2019). Spatially Integrated Social Sciences with Qualitative GIS to Support Impact Assessment in Mining Communities. *Resources*, *8*(1). <https://doi.org/10.3390/resources8010047>
- Li, J., Yan, X., Cao, Z., Yang, Z., Liang, J., Ma, T., & Liu, Q. (2020). Identification of successional trajectory over 30 Years and evaluation of reclamation effect in coal waste dumps of surface coal mine. *Journal of Cleaner Production*, *269*. <https://doi.org/10.1016/j.jclepro.2020.122161>
- Liu, H. Q., & Huete, A. R. (1995). A feedback based modification of the NDVI to minimize canopy background and atmospheric noise. *IEEE Transactions on Geoscience and Remote Sensing*, *33*, 457–465.
- Liu, Y., Xie, M., Liu, J., Wang, H., & Chen, B. (2022). Vegetation Disturbance and Recovery Dynamics of Different Surface Mining Sites via the LandTrendr Algorithm: Case Study in Inner Mongolia, China. *Land*, *11*(6). <https://doi.org/10.3390/land11060856>
- LP DAAC - ASTER Overview*. (n.d.). Retrieved January 30, 2023, from <https://lpdaac.usgs.gov/data/get-started-data/collection-overview/missions/aster-overview/>
- Ma, B., Pu, R., Wu, L., & Zhang, S. (2017). Vegetation Index Differencing for Estimating Foliar Dust in an Ultra-Low-Grade Magnetite Mining Area Using Landsat Imagery. *IEEE Access*, *5*, 8825–8834. <https://doi.org/10.1109/ACCESS.2017.2700474>

- Madasa, A., Orimoloye, I. R., & Ololade, O. O. (2021). Application of geospatial indices for mapping land cover/use change detection in a mining area. *Journal of African Earth Sciences*, 175. <https://doi.org/10.1016/j.jafrearsci.2021.104108>
- Major, D. J., Baret, F., & Guyot, G. (1990). A ratio vegetation index adjusted for soil brightness. *International Journal of Remote Sensing*, 11(5), 727–740. <https://doi.org/10.1080/01431169008955053>
- Maschler, J., Atzberger, C., & Immitzer, M. (2018). Individual Tree Crown Segmentation and Classification of 13 Tree Species Using Airborne Hyperspectral Data. *Remote Sensing 2018, Vol. 10, Page 1218, 10(8)*, 1218. <https://doi.org/10.3390/RS10081218>
- McFeeters, S. K. (1996). The use of the Normalized Difference Water Index (NDWI) in the delineation of open water features. *International Journal of Remote Sensing*, 17(7), 1425–1432. <https://doi.org/10.1080/01431169608948714>
- McKenna, P. B., Lechner, A. M., Phinn, S., & Erskine, P. D. (2020). Remote sensing of mine site rehabilitation for ecological outcomes: A global systematic review. In *Remote Sensing* (Vol. 12, Issue 21, pp. 1–32). MDPI AG. <https://doi.org/10.3390/rs12213535>
- Moderate Resolution Imaging Spectroradiometer (MODIS) - LAADS DAAC*. (n.d.). Retrieved January 16, 2023, from <https://ladsweb.modaps.eosdis.nasa.gov/missions-and-measurements/modis/>
- MODIS Web*. (n.d.). Retrieved January 16, 2023, from <https://modis.gsfc.nasa.gov/data/>
- Mukherjee, J., Mukherjee, J., & Chakravarty, D. (2019). Automated seasonal separation of mine and non mine water bodies from landsat 8 oli/tirs using clay mineral and iron oxide ratio. *IEEE Journal of Selected Topics in Applied Earth Observations and Remote Sensing*, 12(7), 2550–2556. <https://doi.org/10.1109/JSTARS.2019.2895385>
- Mukherjee, J., Mukhopadhyay, J., & Chakravarty, D. (2018). Investigation of Seasonal Separation in Mine and Non Mine Water Bodies Using Local Feature Analysis of Landsat 8 OLI/TIRS Images. *IGARSS 2018 - 2018 IEEE International Geoscience and Remote Sensing Symposium*, 8961–8964.
- Nussbaum, S., & Niemeyer, I. (2009). *International Safeguards and Satellite Imagery* (G. Stein, B. Richter, S. Nussbaum, I. Niemeyer, & B. Jasani, Eds.). Springer Berlin Heidelberg. <https://doi.org/10.1007/978-3-540-79132-4>
- OCP Group - Sustainability Integrated Report*. (2021). [https://ocpsiteprodsa.blob.core.windows.net/media/2022-08/OCP GROUP INTEGRATED REPORT 2021.pdf](https://ocpsiteprodsa.blob.core.windows.net/media/2022-08/OCP_GROUP_INTEGRATED_REPORT_2021.pdf)
- Padmanaban, R., Bhowmik, A. K., & Cabral, P. (2017). A remote sensing approach to environmental monitoring in a reclaimed mine area. *ISPRS International Journal of Geo-Information*, 6(12). <https://doi.org/10.3390/ijgi6120401>
- Pawlik, M., Rudolph, T., Benndorf, J., & Blachowski, J. (2021). Review of vegetation indices for studies of post-mining processes. *IOP Conference Series: Earth and Environmental Science*, 942(1). <https://doi.org/10.1088/1755-1315/942/1/012034>
- Pettorelli, N. (2013). Vegetation indices. In *The Normalized Difference Vegetation Index* (pp. 18–29). Oxford University Press. <https://doi.org/10.1093/acprof:osobl/9780199693160.003.0002>

- Pour, A. B., & Hashim, M. (2014). Alteration mineral mapping using ETM+ and hyperion remote sensing data at Bau Gold Field, Sarawak, Malaysia. *IOP Conference Series: Earth and Environmental Science*, 18(1). <https://doi.org/10.1088/1755-1315/18/1/012149>
- Qi, J., Chehbouni, A., Huete, A. R., Kerr, Y. H., & Sorooshian, S. (1994). A Modified Soil Adjusted Vegetation Index. *REMOTE SENS. ENVIRON.*, 48, 119–126.
- QuickBird-2 - Earth Online*. (n.d.). Retrieved February 2, 2023, from <https://earth.esa.int/eogateway/missions/quickbird-2>
- Radočaj, D., Obhodaš, J., Jurišić, M., & Gašparović, M. (2020). Global open data remote sensing satellite missions for land monitoring and conservation: A review. In *Land* (Vol. 9, Issue 11, pp. 1–24). MDPI AG. <https://doi.org/10.3390/land9110402>
- Richardson, A. J., & Wiegand, C. L. (1977). Distinguishing Vegetation from Soil Background Information. *PHOTOGRAMMETRIC ENGINEERING AND REMOTE SENSING*, 43(12), 1541–1552.
- Rouse J.~W., Jr., Haas, R. ~H., Schell, J. ~A., & Deering, D. ~W. (1974). Monitoring Vegetation Systems in the Great Plains with Erts. In *NASA Special Publication* (Vol. 351, p. 309).
- Sanjerehei, M. M. (2014). Assessment of spectral vegetation indices for estimating vegetation cover in arid and semiarid shrublands. *Range Mgmt. & Agroforestry*, 35(1), 91–100. <https://www.researchgate.net/publication/266969832>
- Satellites | Landsat Science*. (n.d.). Retrieved January 30, 2023, from <https://landsat.gsfc.nasa.gov/satellites/>
- Schaefer, M. T., Lamb, D. W., Ozdogan, M., Baghdadi, N., & Thenkabail, P. S. (2016). A Combination of Plant NDVI and LiDAR Measurements Improve the Estimation of Pasture Biomass in Tall Fescue (*Festuca arundinacea* var. Fletcher). *Remote Sensing 2016, Vol. 8, Page 109*, 8(2), 109. <https://doi.org/10.3390/RS8020109>
- SPOT - Earth Online*. (n.d.). Retrieved January 30, 2023, from <https://earth.esa.int/eogateway/missions/spot>
- Tagebau Profen - MIBRAG mbH*. (n.d.). Retrieved March 2, 2023, from <https://www.mibrag.de/geschaeftsfelder/bergbau/tagebau-profen/>
- Transforming our world: the 2030 Agenda for Sustainable Development | Department of Economic and Social Affairs*. (n.d.). Retrieved January 16, 2023, from <https://sdgs.un.org/2030agenda>
- Tuominen, J., Lipping, T., Kuosmanen, V., & Haapane, R. (2009). Remote Sensing of Forest Health. In *Geoscience and Remote Sensing*. InTech. <https://doi.org/10.5772/8283>
- Tymchuk, I., Malovanyy, M., Shkvirko, O., Chornomaz, N., Popovych, O., Grechanik, R., & Symak, D. (2021). Review of the global experience in reclamation of disturbed lands. *Ecological Engineering and Environmental Technology*, 22(1), 24–30. <https://doi.org/10.12912/27197050/132097>
- Viña, A., Gitelson, A. A., Nguy-Robertson, A. L., & Peng, Y. (2011). Comparison of different vegetation indices for the remote assessment of green leaf area index of crops. *Remote Sensing of Environment*, 115(12), 3468–3478. <https://doi.org/10.1016/j.rse.2011.08.010>

- What are the band designations for the Landsat satellites?* | U.S. Geological Survey. (n.d.). Retrieved January 16, 2023, from <https://www.usgs.gov/faqs/what-are-band-designations-landsat-satellites>
- Wilson, E. H., & Sader, S. A. (2002). Detection of forest harvest type using multiple dates of Landsat TM imagery. *Remote Sensing of Environment*, 80, 385–396. www.elsevier.com/locate/rse
- Wirth, P., & Lintz, G. (2006). Rehabilitation And Development Of Mining Regions In Eastern Germany – Strategies And Outcomes . *MORAVIAN GEOGRAPHICAL REPORTS*, 12(2), 69–82.
- WorldView Series - Earth Online*. (n.d.). Retrieved January 30, 2023, from <https://earth.esa.int/eogateway/missions/worldview>
- WorldView-4 - Earth Online*. (n.d.). Retrieved February 1, 2023, from <https://earth.esa.int/eogateway/missions/worldview-4>
- Woźniak, J., Pactwa, K., Szczęsniewicz, M., & Ciapka, D. (2022). Declaration of the Sustainable Development Goals of Mining Companies and the Effect of Their Activities in Selected Areas. *Sustainability (Switzerland)*, 14(24). <https://doi.org/10.3390/su142416422>
- Xie, Y., Sha, Z., & Yu, M. (2008). Remote sensing imagery in vegetation mapping: a review. *Journal of Plant Ecology*, 1(1), 9–23. <https://doi.org/10.1093/jpe/rtm005>
- Xu, H. (2006). Modification of normalised difference water index (NDWI) to enhance open water features in remotely sensed imagery. *International Journal of Remote Sensing*, 27(14), 3025–3033. <https://doi.org/10.1080/01431160600589179>
- Xue, J., & Su, B. (2017). Significant remote sensing vegetation indices: A review of developments and applications. In *Journal of Sensors* (Vol. 1, pp. 1–17). Hindawi Limited. <https://doi.org/10.1155/2017/1353691>
- Yu, S., Sun, L., Sun, Z., & Wu, M. (2016). Water body extraction and change analysis based on landsat image in Xinjiang coal-mining regions. *2016 IEEE International Geoscience and Remote Sensing Symposium (IGARSS)*, 6229–6232.

List of Figures

Figure 1. Simplified flow chart of a surface mining operations	7
Figure 2. Reflectance of water, soil and vegetation in different wavelengths and Landsat TM channels (Classification Algorithms and Methods, n.d.).....	18
Figure 3. Schematic diagram of the vegetation index trajectory over time at a mine site (Liu et al., 2022)	19
Figure 4. Landsat Level-2 and Level-3 Science Products (Landsat Level-2 and Level-3 Science Products U.S. Geological Survey, n.d.).....	30
Figure 5. Map showing the location of the Profen mine in Germany	33
Figure 6. Map of the Profen mine (Braunkohlengesellschaft mbH MIBRAG & Kappa GmbH, n.d.)	34
Figure 7. A vision of the post-mining landscape at The Profen mine (Braunkohlengesellschaft mbH MIBRAG & Kappa GmbH, n.d.).....	35

Figure 8. Drought intensities in the growing season from April to October (1981-2022) (Dürren 1952 - 2022 (Jährlich) - Helmholtz-Zentrum Für Umweltforschung UFZ, n.d.)	36
Figure 9. Drought magnitudes in the April to October growing season (1981-2022) (Dürren 1952 - 2022 (Jährlich) - Helmholtz-Zentrum Für Umweltforschung UFZ, n.d.)	37
Figure 10. Mining area of Profen with zoning plan (Braunkohlenrevier, n.d.)	38
Figure 11. Location of the post-mining region, study zones and points	39
Figure 12. Average spectral signatures of the 13 tree species (Maschler et al., 2018) ...	40
Figure 13. Mean NDVI values in years 1986-2022	41
Figure 14. Standard deviation of NDVI in years 1986-2022	42
Figure 15. Mean EVI2 values in years 1986-2022.....	43
Figure 16. Standard deviation of EVI2 in years 1986-2022	43
Figure 17. Mean SAVI values in years 1986-2022	44
Figure 18. Standard deviation of SAVI in years 1986-2022.....	44
Figure 19. NDVI value for point in years 1986-2022	45
Figure 20. EVI2 value for point in years 1986-2022	46
Figure 21. SAVI value for point in years 1986-2022.....	46
Figure 22. Difference raster of the NDVI values in 1986-2022.....	47
Figure 23. Difference raster of the EVI2 values in 1986-2022	48
Figure 24. Difference raster of the SAVI values in 1986-2022	48

List of Tables

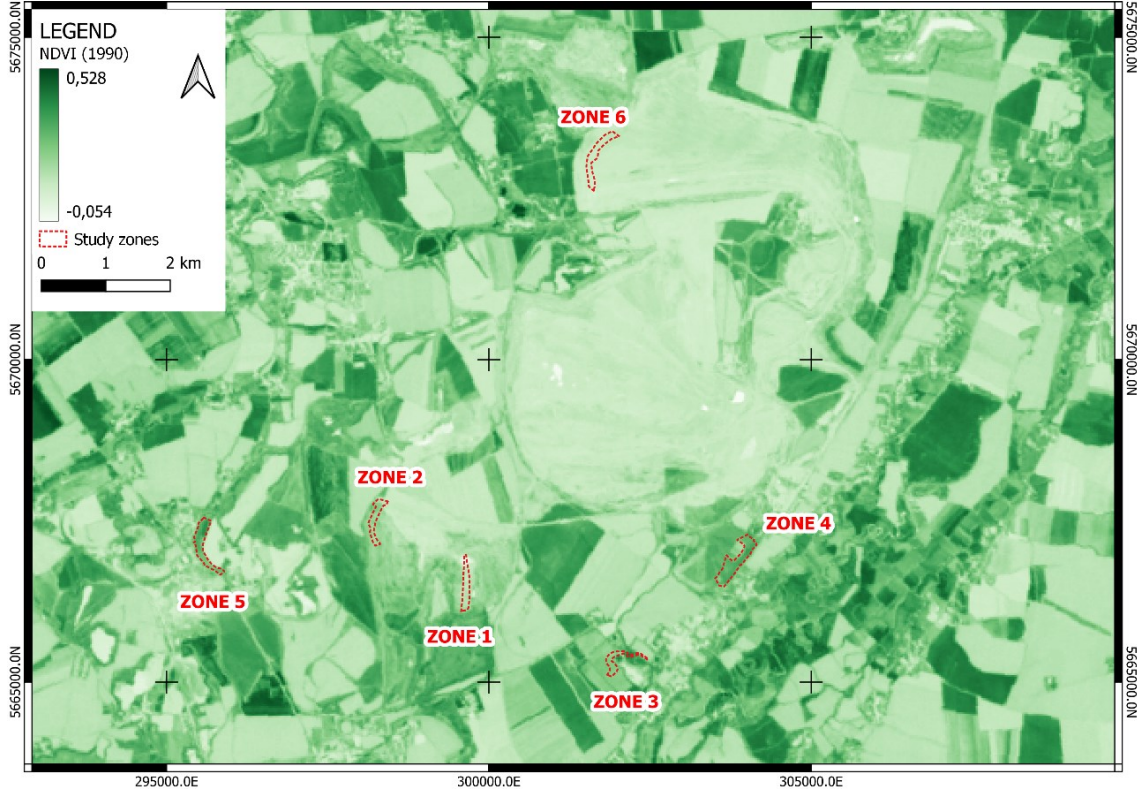
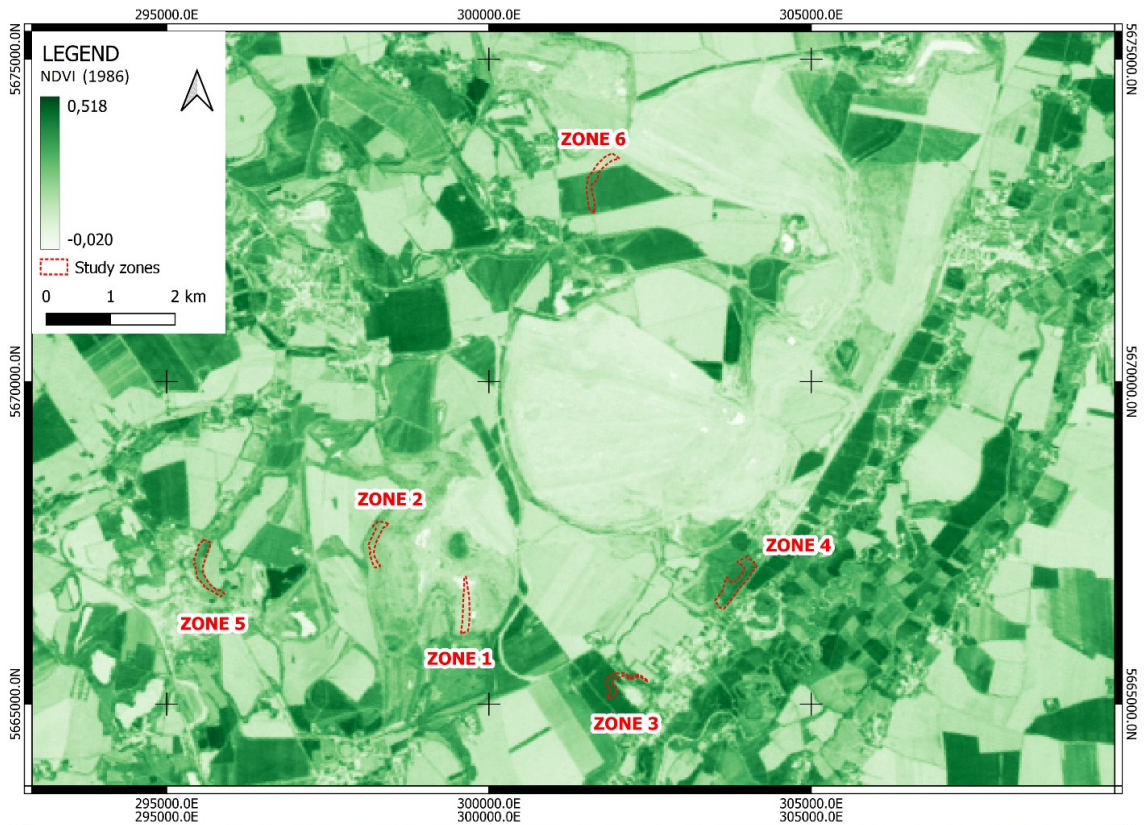
Table 1. Comparison of satellite missions	14
Table 2. Characteristics of spectral bands and spatial resolution of satellite missions...	17
Table 3. Selected vegetation and water indices found in the literature	24
Table 4. Summary of chosen case studies found in recent research publications.....	27
Table 5. Landsat images acquired from 1 June to 31 August in the years 1986-2022 ...	32
Table 6. Summary of vegetation information for study zones	39

List of Appendices

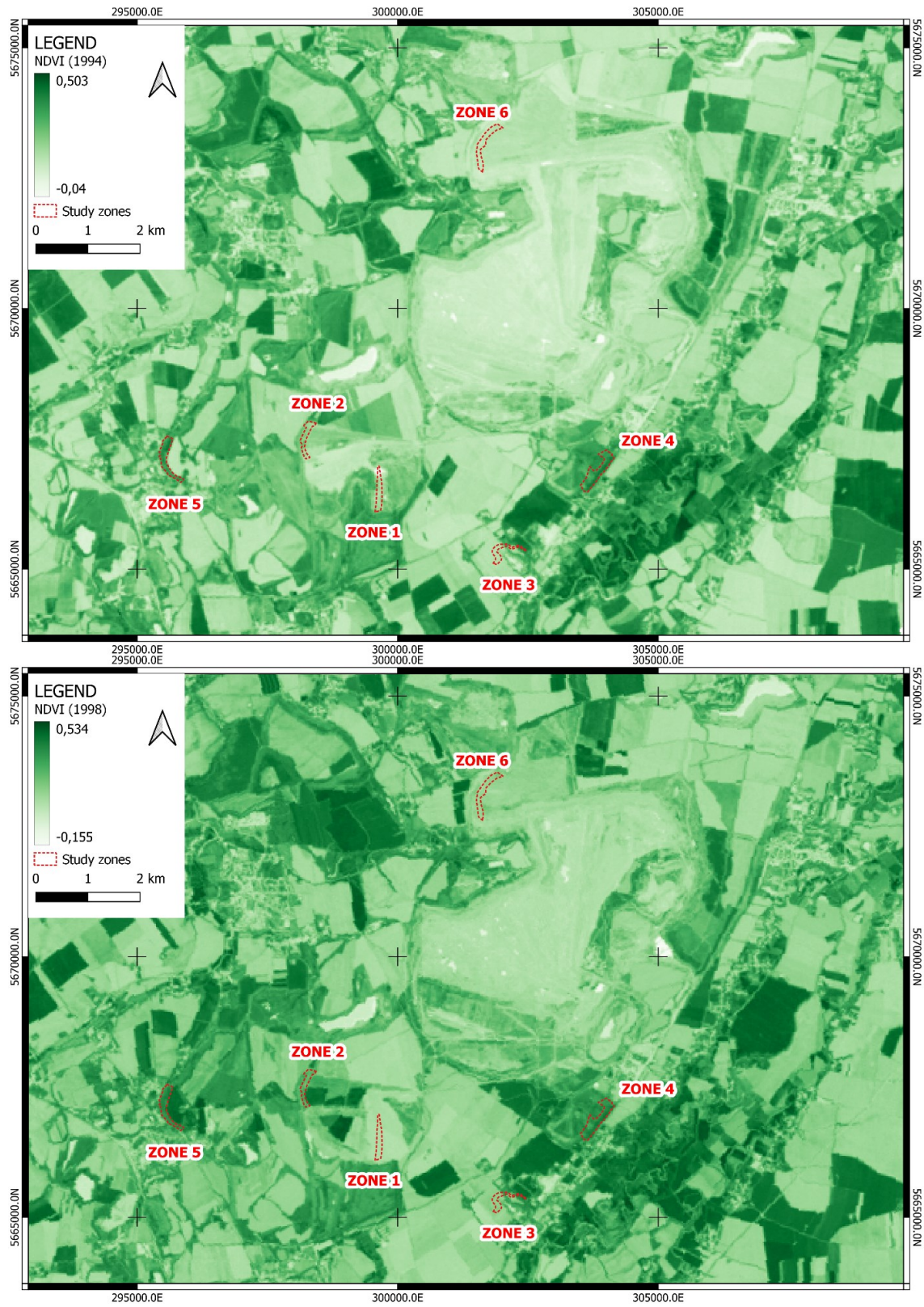
Appendix 1A Map of Profen mine with NDVI values for July 1986 and July 1990
Appendix 1B Map of Profen mine with NDVI values for July 1994 and July 1998
Appendix 1C Map of Profen mine with NDVI values for July 2002 and July 2006
Appendix 1D Map of Profen mine with NDVI values for July 2010 and July 2014
Appendix 1E Map of Profen mine with NDVI values for July 2018 and July 2022
Appendix 2A Map of Profen mine with EVI2 values for July 1986 and July 1990
Appendix 2B Map of Profen mine with EVI2 values for July 1994 and July 1998

Appendix 2C Map of Profen mine with EVI2 values for July 2002 and July 2006
Appendix 2D Map of Profen mine with EVI2 values for July 2010 and July 2014
Appendix 2E Map of Profen mine with EVI2 values for July 2018 and July 2022
Appendix 3A Map of Profen mine with SAVI values for July 1986 and July 1990
Appendix 3B Map of Profen mine with SAVI values for July 1994 and July 1998
Appendix 3C Map of Profen mine with SAVI values for July 2002 and July 2006
Appendix 3D Map of Profen mine with SAVI values for July 2010 and July 2014
Appendix 3E Map of Profen mine with SAVI values for July 2018 and July 2022

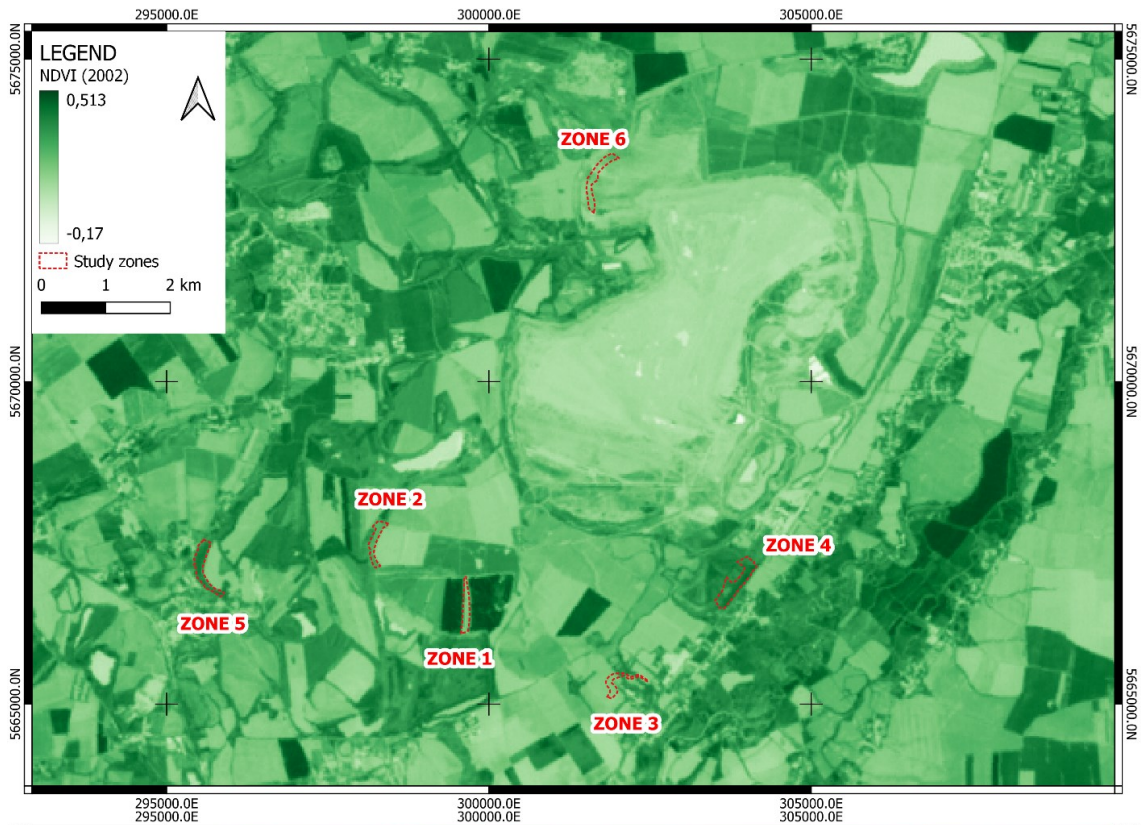
Map of Profen mine with NDVI values for July 1986 and July 1990



Map of Profen mine with NDVI values for July 1994 and July 1998



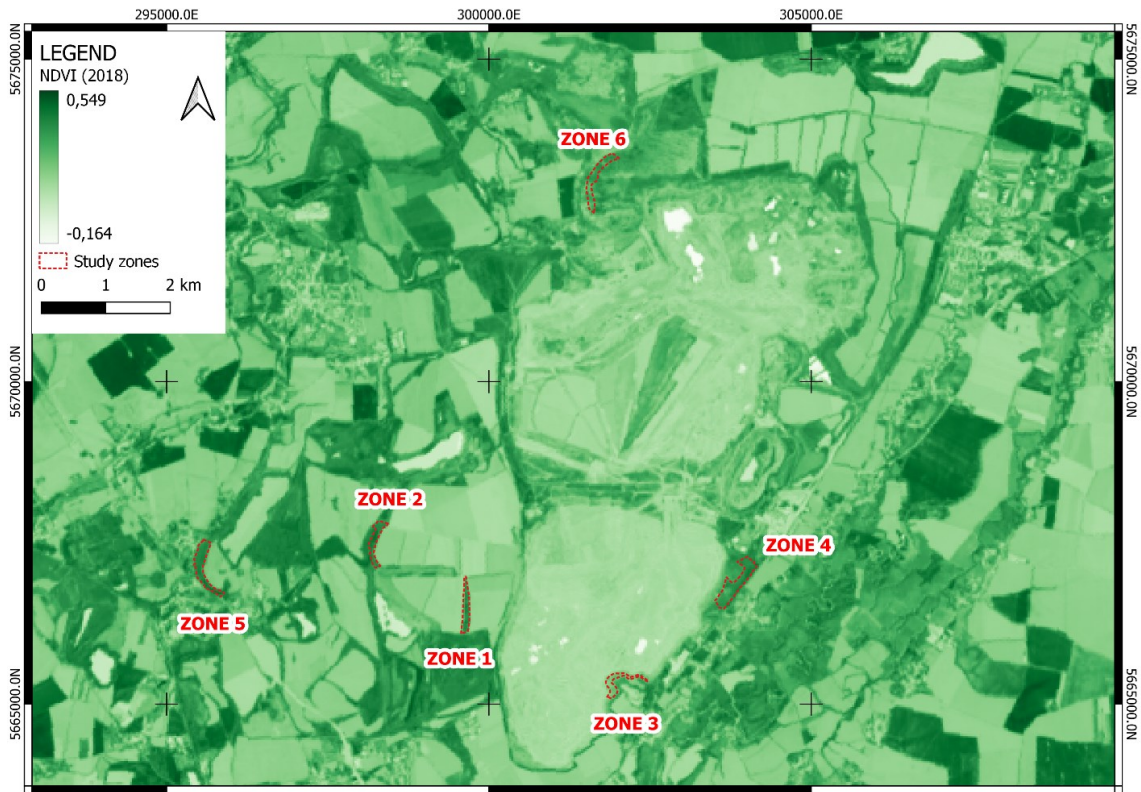
Map of Profen mine with NDVI values for July 2002 and July 2006



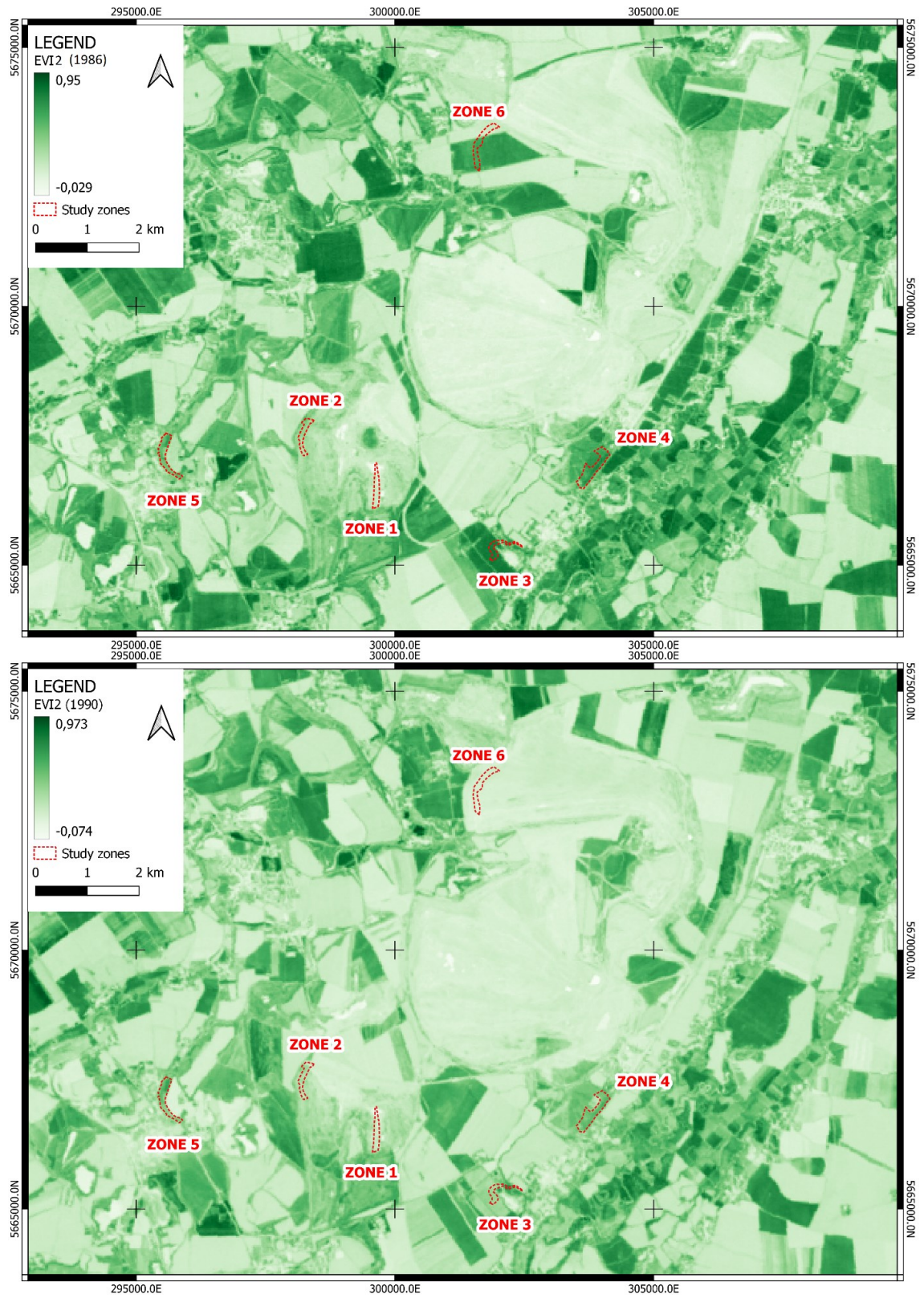
Map of Profen mine with NDVI values for July 2010 and July 2014



Map of Profen mine with NDVI values for July 2018 and July 2022



Map of Profen mine with EVI2 values for July 1986 and July 1990



Map of Profen mine with EVI2 values for July 1994 and July 1998



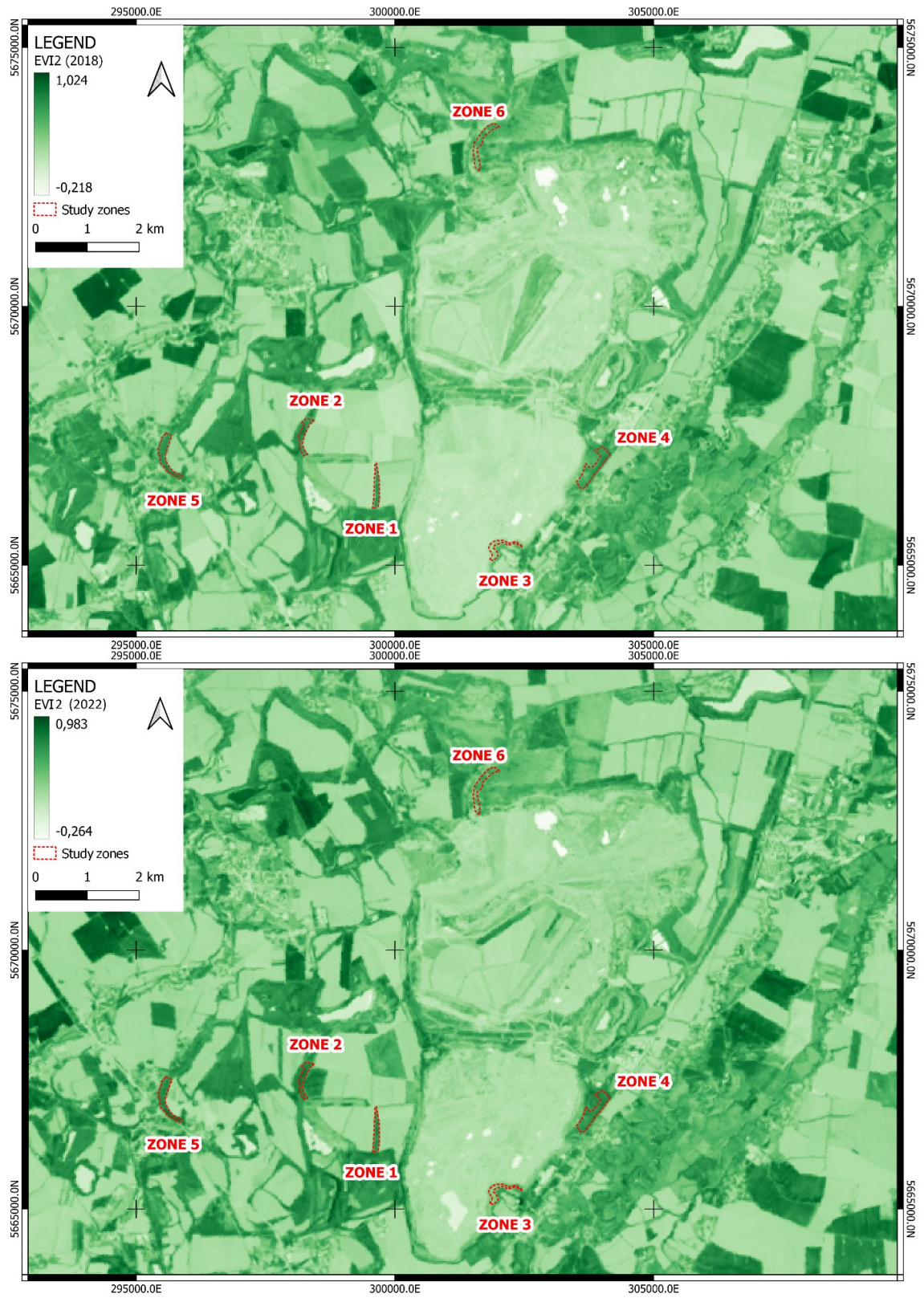
Map of Profen mine with EVI2 values for July 2002 and July 2006



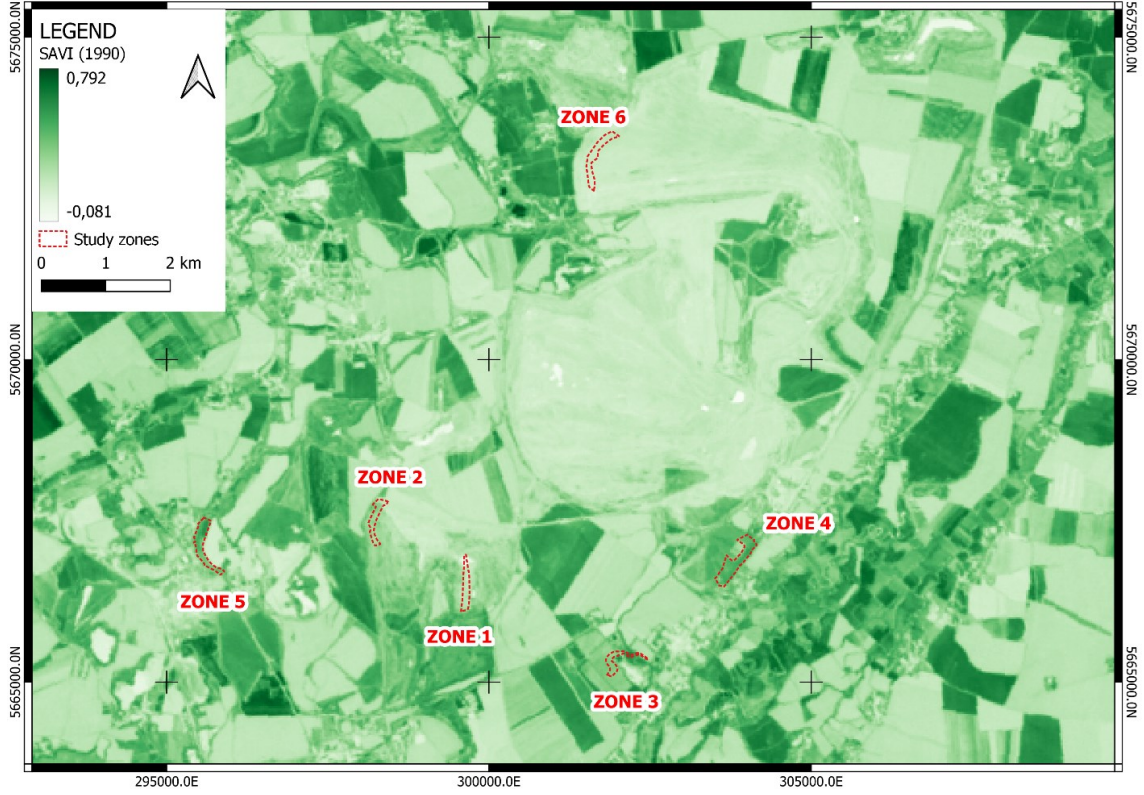
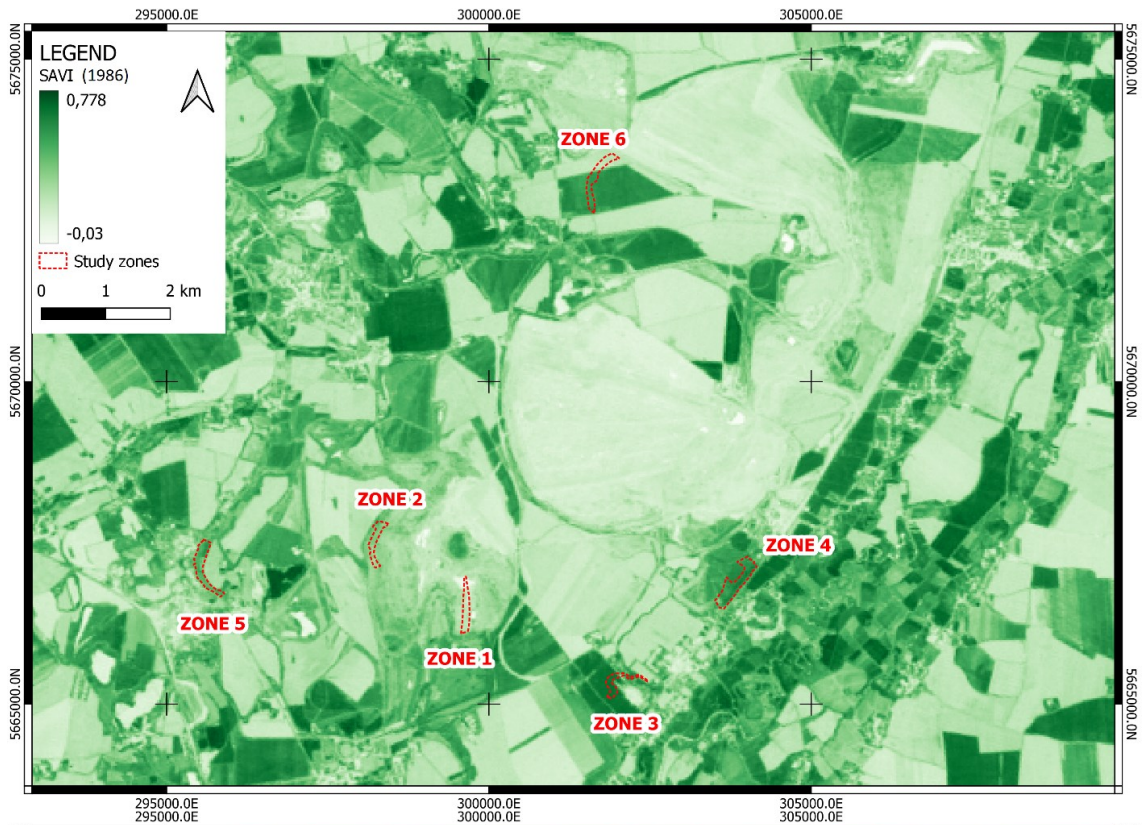
Map of Profen mine with EVI2 values for July 2010 and July 2014



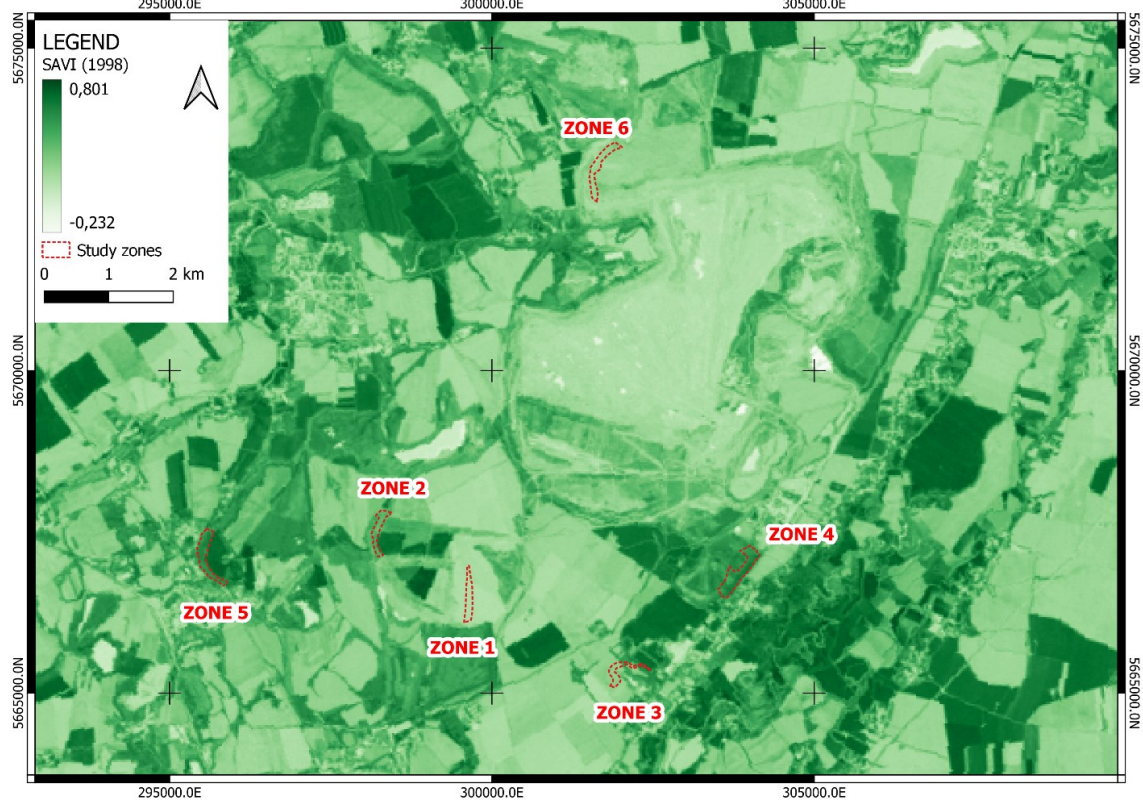
Map of Profen mine with EVI2 values for July 2018 and July 2022



Map of Profen mine with SAVI values for July 1986 and July 1990



Map of Profen mine with SAVI values for July 1994 and July 1998



Map of Profen mine with SAVI values for July 2002 and July 2006



Map of Profen mine with SAVI values for July 2010 and July 2014



Map of Profen mine with SAVI values for July 2018 and July 2022

